

Taming Client Dropout for Distributed Differential Privacy in Federated Learning

Zhifeng Jiang
HKUST

Wei Wang
HKUST

Ruichuan Chen
Nokia Bell Labs

Abstract

Federated learning (FL) is increasingly deployed among multiple clients (e.g., mobile devices) to train a shared model over decentralized data. To address the privacy concerns, FL systems need to protect the clients’ data from being revealed during training and also control the data leakage through trained models when exposed to untrusted domains. Distributed differential privacy (DP) offers an appealing solution in this regard as it achieves an informed tradeoff between privacy and utility without a trusted server. However, existing distributed DP mechanisms work impractically in real world. For instance, to handle realistic scenarios with *client dropout*, these existing mechanisms often make strong assumptions about client participation yet still result in either poor privacy guarantees or unsatisfactory training accuracy.

We present Hyades, a distributed differentially private FL framework that is highly efficient and resilient to client dropout. First, we develop a new privacy accounting technique under the notion of Rényi DP that tightly bounds the privacy loss in the presence of dropout before client sampling in FL. This enables Hyades to set a minimum target noise level in each training round. Second, we propose a novel ‘add-then-remove’ masking scheme to enforce this target noise level, even though some sampled clients may still drop out in the end. Third, we design an efficient secure aggregation mechanism that optimally pipelines communication and computation for faster execution. Evaluation through large-scale cloud deployment shows that Hyades can efficiently handle client dropout in various realistic scenarios, attaining the optimal privacy-utility tradeoff and accelerating the training by up to $2.1\times$ compared to existing solutions.

1 Introduction

Federated learning (FL) [44, 53] allows multiple clients (e.g., mobile and edge devices) to collaboratively train a shared model under the orchestration of a central server. In scenarios where the number of clients is large (e.g., millions of mobile

devices), the server dynamically *samples* a small subset of clients to participate in each training round [16]. The sampled clients download the global model from the server, compute individual local updates using private data, and upload local updates to the server for global aggregation. Throughout the training, no client’s data is exposed directly. FL has been deployed in various domains to enable a multitude of privacy-sensitive AI applications [33, 51, 52, 59, 61, 80].

However, only keeping client data on device is insufficient to preserve data privacy. Recent work shows that sensitive data can still be revealed through message exchanges in FL training [28, 29, 34, 55, 79, 83]. It is also possible, with theoretical and empirical evidences, to infer client’s data from the trained models by leveraging their information memorization capability [19, 58, 70, 74, 82].

Current FL systems often use *differential privacy* (DP) [31] to perturb the aggregate model update in each training round, so as to bound the leakage of individual clients’ data throughout training. Among the three typical DP models (i.e., central [54, 65], local [63], and distributed DP [10, 42, 75]), the *distributed DP* is the most appealing DP model in the FL setting as it: 1) assumes *no trusted server* (as opposed to central DP), and 2) imposes the *smallest noise* given a privacy budget (as opposed to local DP), causing minimum utility loss to trained models. Specifically, given a global privacy budget that should not be exceeded, the system first computes the *minimum random noise* required in each training round to control data leakage. Afterwards, in each round, it samples a subset of clients and applies the target noise, and then each sampled client adds a small portion of the noise to its local update. Together, the aggregate update at the server is perturbed by *exactly* the minimum required noise. In distributed DP, local updates are aggregated using the secure aggregation (SecAgg) protocol [17], which ensures that the (untrusted) server learns no individual updates but the aggregate result.

Existing distributed DP mechanisms, however, face two practical challenges when deployed in real-world FL systems. First, the privacy guarantee of distributed DP can be compromised in the presence of *client dropout*, which can occur

anytime, for instance, due to network errors, low battery, or changes in eligibility, as observed in production [16, 48, 81]. Yet, existing privacy accounting methods are incapable of accounting the privacy loss of client sampling when dropout occurs. The standard technique they use, called privacy amplification via subsampling [78, 84], requires each client to be sampled uniformly with a non-zero probability in each round. For those clients who dropped *before sampling*, they cannot be selected and their effective sampling rate is zero. This invalidates the standard privacy accounting technique, making it unable to plan the allocation of privacy budget in each training round (§2.3). Clients can also drop *after being sampled*. Missing their noise contributions, the aggregate update ends up with insufficient DP protection, thus consuming more privacy budget than originally planned in each round [42]. As the privacy budget runs out quickly, the training has to stop in earlier round, resulting in a significant model utility loss (§8).

Second, in addition to the privacy issues caused by client dropout, the use of SecAgg protocol [17] in distributed DP raises severe efficiency issues. This is because, to ensure secure aggregation, SecAgg performs multi-round communications and heavy cryptographic computations. The overhead of these operations grows quadratically with the number of sampled clients, significantly limiting the scalability of its deployment in practice [16]. In our experiments, SecAgg can take up to 91% of the training time (§2.3). Thus, it is critical to accelerate SecAgg for distributed DP in the FL scenario.

In this paper, we present Hyades, an efficient FL framework that enables dropout-resilient distributed DP in FL. Hyades addresses both the privacy and efficiency issues of distributed DP in an FL system with three key contributions. First, we develop a new *privacy accounting* technique to handle client dropout (§4). Our insight is that having clients dropped *before* client sampling should not increase the exposure of their data. Following this insight, we generalize existing privacy accounting mechanisms in a non-trivial way by allowing clients to have varying sampling rates in a certain interval. We show that the maximum privacy loss is attained when the sampling rate reaches the maximum. This gives a tight analysis of privacy loss in the presence of client dropout under the notion of Rényi DP [57], thus enabling Hyades to accurately plan the privacy budget allocated to each training round.

Second, to ensure that the aggregate model update is perturbed with exactly the minimum required noise regardless of client dropout *after* being sampled, we devise a novel *add-then-remove* approach (§5). Specifically, Hyades first lets each sampled client add excessive noise to its local update, such that the aggregate noise retains sufficient even when many sampled clients drop out in the end. After aggregation, the server removes part of the excessive noise that is over the minimum noise requirement, based on actual client participation. Using Shamir’s secret sharing [69], we ensure that the entire process is dropout-resilient. We further devise an efficient *approximate* noise enforcement scheme that reduces

the complexity of computation and communication without a noticeable utility loss.

Third, to accelerate SecAgg used in distributed DP, we develop an efficient *pipeline execution* scheme (§6). Our scheme optimally divides a client’s update into multiple chunks, and pipelines their computation- and communication-intensive operations (e.g., data encoding and transmission) in SecAgg for maximum acceleration. Our scheme is general and can be used to accelerate other secure aggregation protocols (e.g., [41, 72, 73]) in distributed DP, for which we also provide a generic programming interface in Hyades (§7).

We have implemented Hyades and evaluated its performance with various FL training tasks in a 100-node EC2 cluster that emulates the hardware heterogeneity of client devices (§8). Evaluation results show that the required noise being added to an aggregate model update in Hyades can always be enforced under various client dropout dynamics, while still maximally preserving the model utility. In terms of the end-to-end performance, we show that Hyades’s pipeline execution speeds up the baseline system by up to 2.1×, without impairing other desirable properties such as dropout resilience. Hyades will be open-sourced.

2 Background and Motivation

2.1 Federated Learning and Threat Model

Federated Learning. Federated learning (FL) enables a large number of clients (e.g., millions of mobile and edge devices) to collaboratively build a global model without sharing local data [44, 53]. In FL, a (logically) centralized server maintains the global model and orchestrates the iterative training. At the beginning of each training round, the server randomly samples a subset of available clients as participants [16].¹ The sampled clients perform local training to the downloaded global model using their individual private data and report only the model updates to the server. The server collects the updates from participants until a certain deadline, and aggregates these updates. It then uses the aggregate update (e.g., FedAvg [53]) to refine the global model.

Threat Model. Although client data is not directly exposed in the FL process, a large body of research has shown that it is still possible to reveal sensitive client data from individual updates or trained models via *data reconstruction* or *membership inference* attacks [19, 28, 29, 34, 55, 58, 62, 70, 74, 79, 82, 83]. For example, an adversary can accurately reconstruct a client’s training data from its gradient updates [55, 62, 83]; an adversary can also infer from a trained language model whether a client’s private text is in the training set [19, 74]. We aim to defend against both data reconstruction and membership inference attacks by controlling the exposure of individual client’s data in the training process.

¹Many recent studies suggest using more advanced sampling algorithms in FL to improve the time-to-accuracy performance [20, 39, 45, 49].

We assume that both the centralized server and participating clients are *honest but curious*. They faithfully follow the specified training process; while doing so, they are eager to pry on the others’ data by means of membership or reconstruction attacks. We do not assume collusion between the server and clients or among clients themselves. Having said that, our work can be easily extended to provide the same privacy guarantee with negligible extra utility loss when the collusion is “mild” (which is typically the case in reality). We will discuss this extension in §9.

2.2 Differential Privacy

Differential privacy (DP) [26, 30, 31] is known to effectively address the reconstruction and membership attacks in our threat model. In a nutshell, the two classes of attacks work by finding data entries that make the observed messages (e.g., local updates and their aggregates) more likely. To prevent these attacks, DP ensures that no specific data entry (or more strongly in FL, client participation) can noticeably increase the likelihood of the messages. This guarantee is captured by a pair of parameters, ϵ and δ [31]. Given any two neighboring training sets D and D' that differ only in the inclusion of a single client’s data, the aggregation procedure f is (ϵ, δ) -differentially private if, for any set of output R , we have

$$\Pr[f(D) \in R] \leq e^\epsilon \cdot \Pr[f(D') \in R] + \delta. \quad (1)$$

In other words, a change in a client’s participation yields at most a multiplicative change of e^ϵ in the probability of any output, except with probability $\delta \in [0, 1]$. Intuitively, smaller ϵ and δ indicate a stronger privacy guarantee.

A key property of DP is composition which, in its basic form, states that the process of running an (ϵ_1, δ_1) -DP and (ϵ_2, δ_2) -DP computation on the same dataset is $(\epsilon_1 + \epsilon_2, \delta_1 + \delta_2)$ -DP. This allows one to account for the privacy loss resulting from a sequence of DP-computed outputs, such as the release of multiple aggregate updates in FL. Tighter (i.e., sublinear) analysis of cumulative privacy loss can further be achieved with the notion of Rényi DP [57], which we will use in this work with more details given in §4.

Central DP and Local DP. A straightforward way to apply DP in FL is to let the server add DP-compliant noise to the aggregate update, known as the *central DP* scheme [44]. However, in central DP, the server must be trusted as it has direct access to the (unprotected) aggregate update. While the server may establish a trusted execution environment (TEE) [12, 37] with hardware support, it is still vulnerable to various recent attacks, e.g., side-channel attacks [22, 77]. An alternative DP scheme is *local DP*, in which each sampled client adds DP noise to perturb its local update before contacting the server. As long as the noise added by a client is sufficient for a meaningful DP guarantee on its own, its privacy is preserved regardless of the behavior of the other clients or the server.

This, however, results in excessive accumulated noise in the aggregate update, significantly harming the model utility [42].

Distributed DP. Compared to central and local DP, *distributed DP* offers an appealing solution in FL scenarios as it: 1) requires no trusted server, and 2) imposes the smallest noise given a privacy budget. This is achieved by simulating a trusted third party via cryptographic protocols. In distributed DP, a privacy goal is specified as a global privacy budget (ϵ_G, δ_G) , which can be viewed as a non-replenishable resource that is consumed by each release of an aggregate update. Ideally, by the time when the training completes, the remaining budget should be zero, so as to meet the privacy goal at the expense of minimum DP noise and model utility loss. This requires the system to perform *offline noise planning* ahead of time to determine the minimum required noise that should be added to the aggregate update in each training round to control privacy loss.

The system then proceeds to *online noise enforcement*. In each training round, it evenly splits the noise adding task to all sampled clients. Each of them slightly perturbs its update by adding an even share of the minimum required noise. The clients then mask their updates and send them to the server using the secure aggregation (SecAgg) protocol [17], which ensures that the server learns nothing but the aggregate update that is perturbed with exactly the minimum required noise. Note that, besides the commonly-used SecAgg, the distributed DP can also be implemented using alternative approaches (e.g., secure shuffling [15, 23, 32]). In this paper, we focus on the approaches using SecAgg, given their popularity in FL.

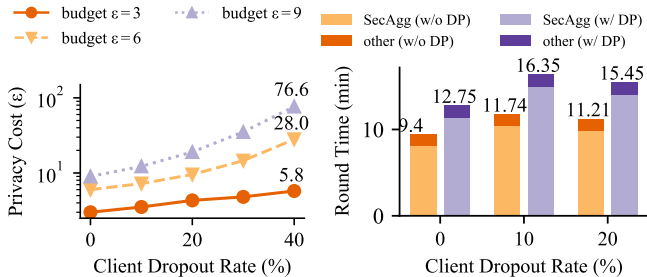
2.3 Practical Issues of Distributed DP

While in theory, distributed DP can achieve an appealing privacy-utility tradeoff, its deployment in real-world systems is impeded by significant practical issues.

2.3.1 Privacy Issues Caused by Client Dropout

In an FL training, *client dropout* can occur anytime due to low battery, poor connections, or switching to a metered network. The prevalence of client dropout, which has been widely observed in real-world systems [16, 48, 81], raises two privacy issues in distributed DP.

Client Dropout before Sampling. The key to offline noise planning is to account the privacy loss at a certain noise level, which enables the system to search the minimum required noise under a privacy budget. Existing privacy accounting methods, however, are incapable of handling client dropout. This is because they use a standard technique called *privacy amplification via subsampling* [8], which was proposed for the traditional data releasing scenario where data is centralized and can be sampled uniformly. When applied to FL scenarios, it essentially requires clients to be sampled uniformly with a nonzero probability in each round [78, 84]. However,



(a) After-sampling dropout compromises the privacy guarantee. (b) SecAgg dominates the runtime of a training round.

Figure 1: Training a ResNet-18 model over CIFAR-10 dataset with distributed DP in an EC2 cluster (settings given in §8.1).

clients who dropped *before* the sampling takes place cannot be selected as participants, and their effective sampling rate is zero. It is for this reason that existing privacy accounting methods cannot be applied, making the system unable to plan the minimum required noise in each round.

Client Dropout after Sampling. Even if the minimum required noise could be accurately planned ahead of time, its enforcement can still be compromised when clients drop *after* being sampled. Without their noise contributions, the total noise added to the aggregate update falls below the minimum required level, leading to increased data exposure that forces the system to consume more privacy budget than originally planned for each round. Should the system follow the original training plan (e.g., completing the training after a certain number of rounds), the cumulative privacy loss inevitably exceeds the global privacy budget [42].

To illustrate this problem, we ran experiments in an EC2 cluster in which 100 clients jointly train a ResNet-18 [8] model over the CIFAR-10 dataset [46]. The detailed setting is given in §8.1. At the beginning of each round, clients are all available and uniformly sampled with probability of 0.16. After being sampled, we let the selected clients randomly drop with a configurable rate. Figure 1a shows the final achieved privacy guarantee when the training completes in 150 rounds with varying dropout rates from 0% to 40%, under three privacy budgets. As the dropout rate increases, more clients’ data gets exposed during training, leading to a larger privacy cost (i.e., larger deficit beyond the target privacy budget). One potential fix to this issue is to early stop the training when the privacy budget runs out. However, this inevitably harms the model accuracy. In our experiments (§8.2), early stop can lose up to 82% of the training rounds, reducing the model accuracy by up to 30% compared to non-private training.

2.3.2 Performance Issue Caused by Secure Aggregation

In addition to the privacy issues caused by client dropout, the SecAgg algorithm [17] used in distributed DP creates a severe performance bottleneck. Specifically, to ensure that

the server learns no individual update from any client but the aggregate update only, SecAgg lets clients synchronize secret keys and use them to generate zero-sum masks. This involves extensive use of pairwise masking and secret sharing, incurring high complexity in both computation and communication (Appendix A). To quantify the performance impact of SecAgg, we refer to Figure 1b which shows the breakdown of the average runtime of one training round in the previous experiment with varying dropout rates. For comparison, we also ran the experiment with SecAgg but add *no* DP noise to the aggregate update. In all experiments with and without DP, the SecAgg cost dominates, accounting for 86-91% of the training time in each round.

Given the high complexity of SecAgg, many alternative algorithms have been proposed for efficient secure aggregation [14, 24, 41, 72, 73]. Yet, none of them could fully replace SecAgg. For example, one desirable property of SecAgg is to ensure that the aggregate update is correctly computed and decoded provided that the number of dropped clients does not exceed a specified threshold. However, algorithms such as SecAgg+ [14], CCESA [24], FastSecAgg [41], and TurboAgg [72] all trade this property for efficiency [73]. Although this may not be a problem for the recent LightSecAgg [73], its communication complexity varies depending on the choice of hyperparameters, which can become prohibitive in practical settings.

3 Hyades Overview

We design Hyades, an efficient FL framework that enables dropout-resilient distributed DP. We first give an overview of Hyades, including its design goals and architecture.

Design Goals. Hyades aims to achieve three design goals, thereby addressing the aforementioned privacy and performance issues of distributed DP in FL.

1) *Resilience to before-sampling dropout:* Given a global privacy budget, the system should optimally determine the minimum required noise in each round before the training starts. Hyades achieves this goal with a new privacy accounting method that tightly bounds the privacy loss at a certain noise level in the presence of client dropout before sampling (§4).

2) *Resilience to after-sampling dropout:* In each round, the system should ensure the minimum required noise is exactly added to the aggregate updates, regardless of client dropout after being sampled. Hyades achieves this with a novel ‘add-then-remove’ approach. It lets each client add excessive noise to its local update to tolerate dropout even in the worst case. Part of the excessive noises over the minimum requirement is then removed based on the actual client participation (§5).

3) *High efficiency of SecAgg:* Given the high complexity of SecAgg and its dominance in training time, the system should optimize the SecAgg operations to mitigate the per-

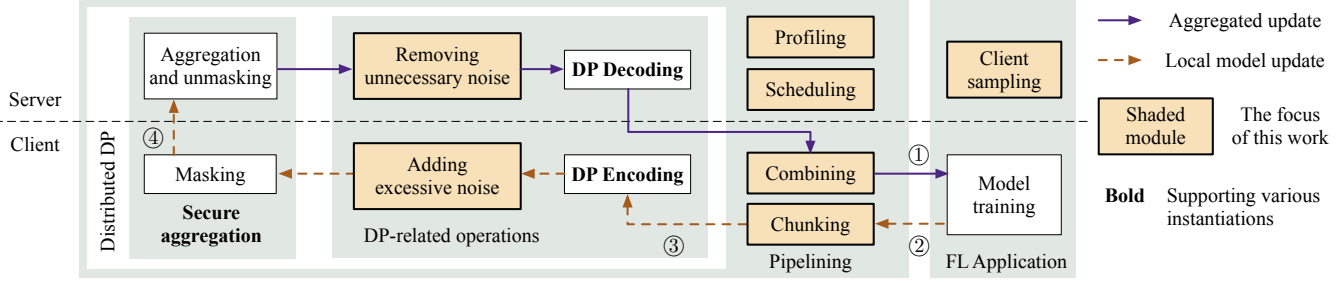


Figure 2: An overview of Hyades’s architecture and how it fits in the existing FL workflow.

formance bottleneck. Hyades achieves this with an efficient pipeline execution scheme that judiciously partitions the local update of a client into chunks and pipelines their processing by overlapping computation and communication for maximum acceleration (§6).

Architecture. Hyades is a practical and efficient distributed differentially private FL framework with new implementations on both the server and clients. Figure 2 shows how Hyades fits in the existing FL workflow. ① *Client sampling and training*: at the beginning of each round, the server randomly samples a subset of available clients as participants. The sampled clients then fetch the global model from the server and compute local updates using their individual private data. ② *Pipeline preparation*: for each participant, the server profiles its processing speed and comes up with an optimal pipeline execution plan. Following the plan, the client chunks the local update for pipelined SecAgg. ③ *Client processing*: for each update chunk, the client perturbs it with the standard DP encoding scheme and our ‘add-then-remove’ noise enforcement approach. The perturbed chunk is further masked following the SecAgg protocol. ④ *Server-side aggregation*: the server aggregates and unmaskes the received update chunks and also removes part of their excessive DP noises to ensure that the residual noise stays at the minimum required level. The server then uses each aggregated update chunk to refine the respective part of the global model.

4 Dropout-Resilient Privacy Accounting

We design a new privacy accounting approach for a tight analysis of privacy loss subject to client dropout before sampling. We then use it to determine the minimum noise required in each training round to control data leakage within the privacy budget. Our approach is built on the notion of Rényi DP.

A Primer on Rényi DP. Rényi DP [57] is an alternative DP notion that gives a tighter privacy analysis than the traditional (ϵ, δ) -DP. Recall in Equation (1) that (ϵ, δ) -DP bounds the δ -approximate max-divergence [68] in the output distribution of a randomized algorithm subject to a small change in input. Rényi DP, expressed with two parameters (α, ϵ) , upper-bounds the output’s Rényi divergence – a measure of

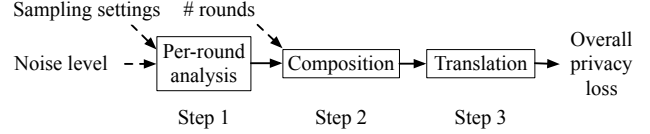


Figure 3: The procedure of privacy accounting in FL.

distance between two distributions – by a small ϵ when the training set differs only in the inclusion of a single client’s data, i.e., $\text{RényiDivergence}_\alpha(f(D), f(D')) \leq \epsilon$, where $\alpha > 1$ is a parameter of Rényi divergence.

Rényi DP has two important properties, which we briefly describe while giving the math details in Appendix B.

1. For every value of α , there is a *direct translation* from Rényi DP to (ϵ, δ) -DP: $(\alpha, \epsilon - \frac{\log(1/\delta)}{\alpha-1})$ -Rényi DP implies (ϵ, δ) -DP for any value of $\epsilon > 0$, $\delta \in (0, 1]$, and $\alpha > 1$. This means that Hyades can use Rényi DP internally while exposing the same (ϵ, δ) -DP guarantee externally.
2. Like (ϵ, δ) -DP, Rényi DP can also be *additively composed*. That is, running an (α, ϵ_1) -Rényi DP and an (α, ϵ_2) -Rényi DP computation on the same dataset is $(\alpha, \epsilon_1 + \epsilon_2)$ -Rényi DP. Yet, when translated to (ϵ, δ) -DP, the privacy loss accounted with Rényi DP is usually *tighter* (i.e., sublinear) than that derived directly with (ϵ, δ) -DP, as Rényi DP utilizes the properties of the used DP mechanism (which affects the particular relationship between ϵ and α , denoted by $\epsilon(\alpha)$), while (ϵ, δ) -DP does not.

Privacy Accounting in FL. Privacy accounting plays a key role in determining the minimum required noise that should be added in each training round. Figure 3 shows how privacy accounting in FL can be done in three steps:

1. Given a noise level (parameterized by the variance σ^2) and the client sampling rate, compute the privacy loss in the notion of Rényi DP for one training round.
2. Given the target number of training rounds, compute the cumulative privacy loss using the composition theory.
3. Translate the privacy loss expressed in Rényi DP into the traditional notion of (ϵ, δ) -DP.

Among all three steps, the main challenge lies in Step 1, as the standard theoretical tool used in privacy accounting (i.e., privacy amplification via subsampling [78, 84]) assumes

uniform client sampling, which is not the case in FL given that clients can drop out before the sampling takes place (§2.3.1).

Dropout-Resilient Privacy Accounting. We develop a new theoretical tool for privacy accounting in Step 1 without assuming the uniform sampling. In particular, we consider a *heterogeneous* sampling process in which clients are sampled independently with non-uniform probabilities ranging from 0 to $\gamma < 1$. More formally, we have the following definition:

Definition 1 (HeteroPoissonSample). *Given a client set C and the sampling probability bound $\gamma \in [0, 1)$, the process $\text{HeteroPoissonSample}(C, \gamma)$ outputs a subset of clients $\{c_i \in C \mid \xi_i = 1\}$ by sampling $\xi_i \sim \text{Bernoulli}(\gamma_i)$, where $\gamma_i \in [0, \gamma]$.*

This HeteroPoissonSample process captures the scenario where clients are uniformly sampled with probability γ but some may drop out before sampling. For those dropped clients, their sampling rate is 0 (i.e., $\gamma_i = 0$).

We next bound the privacy loss in the above sampling process. Intuitively, the privacy loss reaches the maximum when clients are uniformly sampled with probability γ . This is because having a client with less chance of being sampled (i.e., $\gamma_i < \gamma$) should neither increase the data exposure of its own nor the others'. Following this intuition, we derive a tight bound of the privacy loss in HeteroPoissonSample with the following theorem, which generalizes the result of uniform sampling (i.e., Theorem 5 in [84]) in a non-trivial way:

Theorem 1. *Let f be a perturbation algorithm that is $(\alpha, \epsilon(\alpha))$ -Rényi DP and g be the function composition $f(\text{HeteroPoissonSample}(C, \gamma))$. For any integer $\alpha \geq 2$, the privacy loss of g is tightly bounded by*

$$\epsilon_g(\alpha) \leq \frac{1}{\alpha-1} \log \left\{ (1-\gamma)^{\alpha-1} (\alpha\gamma - \gamma + 1) + \binom{\alpha}{2} \gamma^2 (1-\gamma)^{\alpha-2} e^{\epsilon(2)} + 3 \sum_{l=3}^{\alpha} \binom{\alpha}{l} (1-\gamma)^{\alpha-l} \gamma^l e^{(l-1)\epsilon(l)} \right\}. \quad (2)$$

For ease of notation, we denote the right-hand side of the above inequality (2), i.e., the upper bound, as $F(\gamma)$. We give a proof sketch and refer to Appendix C for the complete proof.

Proof Sketch. Recall that Rényi DP bounds the Rényi divergence between the output distributions with and without a client i 's participation, namely $g(D_i)$ and $g(D_{-i})$. Our goal is to prove that $\text{RényiDivergence}_{\alpha}(g(D_i), g(D_{-i})) \leq F(\gamma)$ and $\text{RényiDivergence}_{\alpha}(g(D_{-i}), g(D_i)) \leq F(\gamma)$ for any i .

The key to our proof (see Appendix C) is to show that $F(\cdot)$ monotonically decreases. We therefore have $F(\gamma_i) \leq F(\gamma)$ for all $\gamma_i \leq \gamma$. Combining this monotonicity with the fact that $\text{RényiDivergence}_{\alpha}(g(D_i), g(D_{-i})) \leq F(\gamma_i)$ and $\text{RényiDivergence}_{\alpha}(g(D_{-i}), g(D_i)) \leq F(\gamma_i)$ for any client i (established by Theorem 5 in [84]), we show that Equation (2) holds and conclude the proof. \square

Theorem 1 enables a tight analysis of privacy loss at a certain noise level in one round without worrying about client dropout before sampling, thereby facilitating the aforementioned Step 1 of privacy accounting in FL (Figure 3). Following the remaining accounting procedure (Steps 2 and 3), Hyades accounts the cumulative privacy loss throughout training when a certain noise level is enforced in each round. This essentially enables *offline noise planning* before the training starts (§2.2), in which Hyades searches the minimum noise required, denoted by σ_*^2 , in each of the T training rounds subject to a global privacy budget (ϵ_G, δ_G) by solving

$$\sigma_*^2 = \arg \min_{\sigma^2} \|\text{RDP2DP}(T \cdot F(\gamma), \delta_G) - \epsilon_G\|, \quad (3)$$

where $\text{RDP2DP}(x, y)$ translates a Rényi DP bound x to a bound on ϵ in the (ϵ, δ) -DP notion, given that $\delta = y$.

5 Dropout-Resilient Noise Enforcement

Once the target noise level is set for each training round, it should be strictly enforced. In this section, we describe a novel ‘add-then-remove’ noise enforcement approach that is resilient to the after-sampling client dropout (§5.1) as well as its efficient approximation (§5.2).

5.1 Add-then-Remove Noise Addition

Problem Description. Without loss of generality, we assume that the random noise distribution $\chi(\sigma^2)$ used in DP is *closed under summation* with respect to the variance σ^2 . That is, given two noises $X_1 \sim \chi(\sigma_1^2)$ and $X_2 \sim \chi(\sigma_2^2)$, where X_1 and X_2 are independent, we have $X_1 \pm X_2 \sim \chi(\sigma_1^2 + \sigma_2^2)$. For example, both Gaussian and Skellam [10] distributions have this property. We start with a formal description of the original noise addition process in distributed DP.

Definition 2 (Orig). *Given the set of sampled clients S and the target noise level σ_*^2 in a certain round, Orig lets each client $c_j \in S$ perturb its update Δ_j by adding noise $n_j \sim \chi(\sigma_*^2/|S|)$ and upload the result $\tilde{\Delta}_j = \Delta_j + n_j$ to the server for aggregation.*

The problem of Orig, as described in §2.3, is that when some clients drop after being sampled, their noise contributions are missing; therefore, the eventual noise aggregated at the server will be insufficient. A simple fix is to let the server add back the missing noise contributed by the dropped clients [42]. However, this is not viable under our threat model as the curious server may infer clients’ data from the insufficiently perturbed aggregate result.

Our Key Idea. Instead of letting the server add back the missing noise, we let sampled clients first *add excessive noise* so that the aggregate noise at the server always remains sufficient even if a large number of participants drop out. We

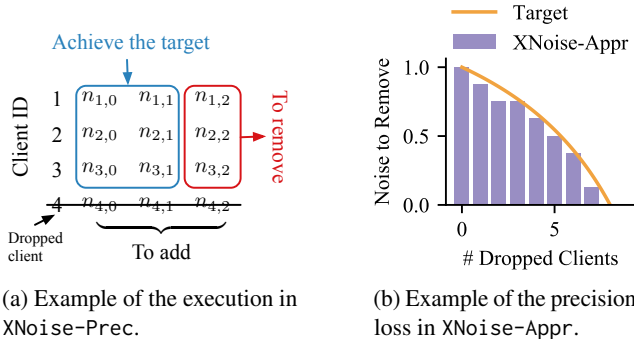


Figure 4: XNoise-Prec precisely enforces the target noise, while XNoise-Appr trades precision for scalability.

then let the server *remove part of the excessive noise* that is over the target level for model utility. Hyades facilitates this ‘add-then-remove’ approach in the existing FL workflow. We next describe its design which addresses two practical issues:

- How much excessive noise should each sampled client add, and how much noise should the server remove in the end based on the actual dropout outcome?
- Given that clients may drop anytime in the middle of noise enforcement, how should the server ensure a correct enforcement result?

Noise Addition and Removal. The amount of excessive noise added by the sampled clients depends on the system’s *tolerance* to their dropout, which is a configurable parameter specified by the FL developer. More formally, let S be the set of sampled clients in a certain training round, among whom the system can tolerate up to t dropouts. Let σ_*^2 be the target noise level in each round. To meet this noise level even in the worst case, Hyades lets each client add an excessive noise at the level of $\frac{\sigma_*^2}{|S|-t}$. In doing so, even if there are t clients dropped after being sampled, the total noise contributed by the remaining $|S| - t$ clients is still sufficient at the target level.

When there are fewer than t clients dropped after being sampled, the aggregate noise at the server exceeds the target level; thus, part of the excessive noise needs to be removed for model utility. Let D denote the set of clients dropped after being sampled, where $D \subset S$ and $|D| \leq t$. The amount of excessive noise that should be removed by the server is:

$$l_{\text{ex}} = \underbrace{(|S| - |D|) \frac{\sigma_*^2}{|S| - t}}_{\text{Actual noise level}} - \sigma_*^2 = \frac{t - |D|}{|S| - t} \sigma_*^2. \quad (4)$$

Intuitively, the more clients dropped after being sampled, the less excessive noise gets removed from the aggregate update.

Hyades uses a carefully-designed noise addition and removal scheme for an exact control of noise enforcement. Specifically, it lets each client $c_i \in S$ decompose the intended excessive noise $n_i \sim \chi(\frac{\sigma_*^2}{|S|-t})$ into $t + 1$ components, i.e., $n_i =$

$\sum_{k=0}^t n_{i,k}$, where $n_{i,0} \sim \chi(\frac{\sigma_*^2}{|S|})$ and $n_{i,k} \sim \chi(\frac{\sigma_*^2}{(|S|-k+1)(|S|-k)})$ for $k = 1, 2, \dots, t$. These noise components are constructed in a way such that when there are $|D|$ clients dropped after being sampled, the noise components $n_{i,k}$ contributed by the remaining clients $c_i \in S \setminus D$ with index $k > |D|$ become excessive and should be removed by the server. One can verify that the aggregate of these removed components is exactly l_{ex} , i.e., $\sum_{c_i \in S \setminus D} \sum_{k=|D|+1}^t n_{i,k} \sim \chi(l_{\text{ex}})$. We next formalize this noise enforcement process.

Definition 3 (XNoise-Prec). *In each training round, a sampled client $c_i \in S$ adds the intended excessive noise to its update Δ_i and sends the perturbed result $\tilde{\Delta}_i = \Delta_i + \sum_{k=0}^t n_{i,k}$ to the server. Among these sampled clients, a subset D has dropped and their updates are missing, where $|D| \leq t$. The server calculates the aggregate update $\tilde{\Delta} = \sum_{c_i \in S \setminus D} \tilde{\Delta}_i$ and then removes all the excessive noise components contributed by the remaining clients (known as survivals) to enforce the target noise level, i.e., $\tilde{\Delta} - \sum_{c_i \in S \setminus D} \sum_{k=|D|+1}^t n_{i,k}$.*

To be concrete, consider the case where 4 clients are sampled in a round, and up to $t = 2$ of them are tolerated to drop. Figure 4a illustrates the noise components that each client adds to their local updates, as well as the noise components removed by the server in case one client drops out.

In the above process, to remove excessive noise, the server needs to collect a number of noise components $\{n_{i,k} \mid k > |D|\}$ from each surviving client $c_i \in S \setminus D$. Directly transferring those components incurs high communication overhead, especially for a sizable model with a large number of parameters. Hyades instead lets clients transfer the *seeds* of the pseudo-random generator (PRG) that are used in generating the requested noise components. As the size of a seed is only a few bytes and does not grow with large models, this greatly reduces the communication overhead.

Dropout-Resilient Noise Removal. Note that some surviving clients can also drop in the middle of seed reporting. Missing their local noise components, the server cannot fully remove the excessive noise added to the aggregate update, ending up with a *higher* noise level than planned. While this does not raise privacy concerns, it unnecessarily harms the model utility. To address this problem, Hyades uses Shamir’s secret sharing scheme [69] for seed reporting: each sampled client secretly shares with others the PRG seeds it uses to generate local noise components. This allows the server to recover any missing local component needed for noise removal, provided that the number of available clients exceeds a certain threshold specified by the secret sharing scheme [69].

Putting It All Together. Figure 5 illustrates how noise enforcement with XNoise-Prec fits in the existing workflow of distributed DP. We summarize the complexity of computation and communication of XNoise-Prec for both the server and a client in Table 1. The complexity analysis is given in Appendix D. As for the privacy guarantee, XNoise-Prec strictly

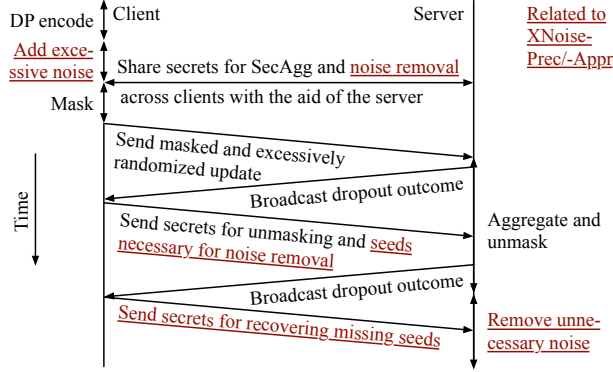


Figure 5: XNoise-Prec/-Appr fits well with the existing workflow of distributed DP.

Table 1: The computational and communication complexity of XNoise-Prec/-Appr, where $|S|$ is the number of sampled clients and d is the model size, measured by the number of model parameters.

Protocol		XNoise-Prec	XNoise-Appr
Comp.	Client	$O(d S + S ^3)$	$O(d \log S + S ^2 \log S)$
	Server	$O(d S ^2 + S ^3)$	$O(d S \log S + S ^2 \log S)$
Comm.	Client	$O(S ^2)$	$O(S \log S)$
	Server	$O(S ^3)$	$O(S ^2 \log S)$

enforces the target noise level under our threat model, as established by Theorem 2. The proof is given in Appendix E.

Theorem 2. XNoise-Prec ensures the noise level in the aggregate update is exactly σ_*^2 , regardless of client dropout.

5.2 Trading Precision for Scalability

While XNoise-Prec ensures exact noise enforcement at the target level, its complexity (Table 1) may limit its scalability when a large number of clients are sampled as participants. We therefore devise an efficient noise control scheme XNoise-Appr that *relaxes* the requirement of exact noise enforcement for improved scalability. Our insight is that the model utility should not have a noticeable degradation when the added noise is only slightly higher than the target level, thanks to machine learning’s error-tolerant nature [64].

We use the same notation as in §5.1. At its core, XNoise-Appr lets each sampled client $c_i \in S$ approximate the intended excessive noise $n_i \sim \chi(\frac{\sigma_*^2}{|S|-t})$ using only $\lceil \log_2 t \rceil + 2$ noise components (as opposed to Xnoise-Prec which decomposes n_i into $t + 1$ components). These noise components are carefully designed as a geometric series with ratio 1/2: after receiving the aggregate update, the server removes certain noise components of the surviving clients, so as to maintain the residual noise at the target level *approximately*. Compared to the exact scheme, the approximate scheme deals with a significantly smaller number of noise components (i.e., $O(\log|S|)$

for each client in XNoise-Appr as compared with $O(|S|)$ in Xnoise-Prec), thus making it much more efficient (Table 1). We formalize the entire process as follows.

Definition 4 (XNoise-Appr). Let $\tau = \lceil \log_2 t \rceil$ and $\eta = \frac{\sigma_*^2 t}{2^\tau |S| (|S| - t)}$. Each client $c_i \in S$ perturbs its update Δ_i by adding $\tau + 2$ noise components, i.e., $\tilde{\Delta}_i = \Delta_i + \sum_{k=0}^{\tau+1} n_{i,k}$, where $n_{i,0} \sim \chi(\sigma_*^2 / |S|)$, $n_{i,1} \sim \chi(\eta)$, and $n_{i,k} \sim \chi(\eta \cdot 2^{k-2})$ for $k = 2, \dots, \tau + 1$. The perturbed update $\tilde{\Delta}_i$ is then sent to the server for aggregation.

After calculating the aggregated update $\tilde{\Delta} = \sum_{c_i \in S \setminus D} \tilde{\Delta}_i$, the server removes from it a collection of noise components contributed by the surviving clients. Specifically, when there is no dropout ($D = \emptyset$), the server removes all $n_{i,k}$ where $k > 0$; otherwise, for each surviving client $c_i \in S \setminus D$, the server removes $n_{i,k}$ where $k \geq 2$ and $b_{k-1} = 1$. Here, $[b_\tau, b_{\tau-1}, \dots, b_1]$ is the τ -bit binary representation of the integer $\lfloor \lambda / \eta \rfloor$, where b_τ is the most significant bit and $\lambda = \frac{(t-D)\sigma_*^2}{(|S|-t)(|S|-|D|)}$.

The following theorem bounds the gap between the target noise level and the one achieved by the XNoise-Appr approximation. The proof is given in Appendix E.

Theorem 3. Given the target noise level σ_*^2 , XNoise-Appr ensures that the approximate noise is within $[\sigma_*^2, \sigma_*^2 + \frac{\sigma_*^2}{|S|-t}]$.

There are two takeaways from Theorem 3. First, the noise imposed by XNoise-Appr is *never* less than the target level, thus controlling the data’s leakage within the privacy budget. Second, the extra noise added by XNoise-Appr is rather small compared to the target noise, within a factor of $\frac{1}{|S|-t} \approx \frac{1}{|S|}$. Figure 4b exemplifies such a subtle noise difference in the case where there are 16 clients, the dropout tolerance is 8, and the target noise level in the aggregate update is 16. As the number of sampled clients increases (larger $|S|$), XNoise-Appr gives a more accurate approximation, and its speedup over XNoise-prec becomes more significant (Table 1). In our experiments, XNoise-Appr causes a negligible accuracy loss compared to XNoise-prec (§8.2).

6 Optimal Pipeline Acceleration

We further devise a pipeline acceleration scheme for the efficiency of our dropout-resilient distributed DP in FL. Our scheme enables pipeline parallelism for SecAgg [17] via the optimal pipeline scheduling of computations and communications at both the server and clients. While we base our design on SecAgg, our pipelining approach is general and can be used to accelerate other secure aggregation protocols in distributed DP.

6.1 Staging Workflow for Pipelined Execution

We identify three types of operations in distributed DP that use different system resources and can be pipelined: 1) s-comp

Table 2: Partitioning the workflow of dropout-resilient distributed DP into stages for pipelined execution.

Step	Operation	Stage (Resource)
1	Clients encode updates.	
2	Clients generate security keys.	
3	Clients establish shared secrets.	1 (c-comp)
4	Clients mask encoded updates.	
5	Clients upload masked updates.	2 (comm)
6	Server deals with dropout.	
7	Server computes aggregate updates.	3 (s-comp)
8	Server updates the global model.	
9	Server dispatches the aggregate.	4 (comm)
10	Clients decode the aggregate.	5 (c-comp)
11	Clients use the aggregate.	

that uses the compute resources (e.g., CPU, GPU, and memory) of the server, 2) c-comp that uses the compute resources of clients, and 3) comm that facilitates server-client communications. Given a distributed DP algorithm and its workflow consisting of a sequence of operations, we group consecutive operations that use the same system resource into a *stage*. As shown in Table 2, the workflow of our distributed DP algorithm using SecAgg can be partitioned into 5 stages for pipelined execution in Hyades. Note that workflow staging is not limited to a particular algorithm, but generally applies to distributed DP using various secure aggregation protocols.

6.2 Pipeline-Parallel Aggregation

Hyades enables *pipeline parallelism* to accelerate the aggregation workflow. It evenly partitions each client’s update Δ_i into m chunks $\Delta_{i,1}, \dots, \Delta_{i,m}$. This divides the global update aggregation into m chunk-aggregation tasks, where the j -th task aggregates the j -th chunks of all clients, i.e., $\sum_i \Delta_i = (\sum_i \Delta_{i,0}) \# \dots \# (\sum_i \Delta_{i,m})$, where $\#$ denotes concatenation. Each chunk-aggregation task follows the same processing stages as in the global aggregation workflow (Table 2). Given that there are m chunk-aggregation tasks, Hyades pipeline-schedules their processing stages to optimally overlap computation and communication. Figure 6 illustrates a pipeline scheduling for distributed DP with 3 chunk-aggregation tasks following the processing stages in Table 2.

Determining the Optimal Number of Chunks. Pipeline-parallel aggregation enables fine-grained scheduling of computation and communication. To achieve the maximum speedup, it is critical to determine the optimal number of chunks, m , used to partition a local update. To this end, we have conducted extensive profiling experiments and established the following performance model that empirically characterizes how the chunk processing time at a stage s , denoted

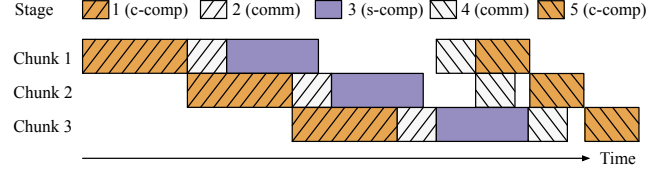


Figure 6: Pipeline scheduling 3 chunk-aggregation tasks for distributed DP in 5 stages as specified in Table 2.

by l_s , is related to m :

$$l_s = \beta_{s,1} \frac{d}{m} + \beta_{s,2} m + \beta_{s,3}, \quad (5)$$

where d is the update size (same as the model size); $\beta_{s,1}$, $\beta_{s,2}$ and $\beta_{s,3}$ are the profiled parameters whose values depend on the hardware configurations and will be used to weigh the different terms described in the following. As indicated in Equation (5), our performance model breaks down the chunk processing time into three terms. The first term is in proportion to the chunk size d/m , which corresponds to the computation/communication overhead; the second term is in proportion to the number of chunks processed in parallel, which measures the delay caused by resource contention and interference; finally, the third term measures a constant processing overhead.

Using the empirical performance model with parameters obtained through online profiling, Hyades can accurately predict the end-to-end aggregation time given the number of chunks. To configure the optimal number, Hyades simply enumerates m within a small range (e.g., $m = 1, 2, \dots, 20$). We refer to Appendix F for a detailed description of this process.

7 Implementation

We have implemented Hyades in 9.3k lines of Python code. Hyades instantiates FL applications with PyTorch [60], and the distributed DP protocol with DSkellam [10] (that employs Skellam for noise mechanism and SecAgg for secure aggregation) following the specified implementation [2, 7]. We make extensive use of multiprocessing and python-redis [6] for efficient computation to support large models, high pipeline parallelism, and a massive number of clients. Our server uses Socket.IO [5] to communicate with clients and nginx [3] to balance the load across I/O processes when handling client requests. The security primitives are built upon standard libraries including Cryptography [1] and PyCryptodome [4]. Hyades will be open-sourced.

Programming Interface. Hyades provides a generic programming interface for developers to implement diverse distributed DP protocols as well as applications that rely on differentially-private aggregate statistics. Specifically, developers can instantiate the abstract classes ProtocolServer and ProtocolClient by overwriting the event handlers to ensemble their distributed DP workflow. This design allows

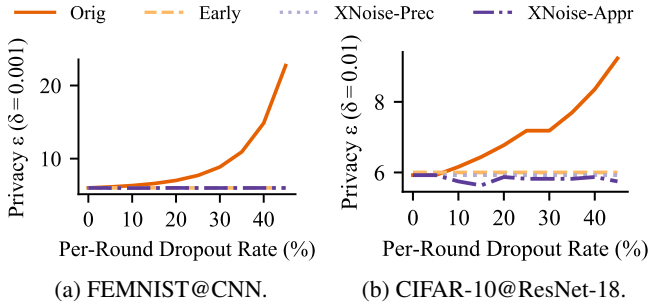


Figure 7: Privacy budget consumption. A larger ϵ corresponds to worse privacy preservation.

developers to focus on the computational logic while delegating the server-client interactions and inter-process communication to Hyades’s backend. Developers can also use other security primitives by overwriting the relevant modules, e.g., `DPHandler`, for plugging in a new noise mechanism. More flexibly, Hyades allows developers to implement other privacy-sensitive applications beyond FL by simply extending the existing `AppServer` and `AppClient` classes with their own data processing logic. Appendix G gives more details.

8 Evaluation

We evaluate Hyades’s effectiveness in various FL training tasks. The highlights of our evaluation are listed as follows.

1. With our dropout-resilient privacy accounting and noise enforcement, Hyades achieves a substantially better privacy-utility tradeoff over alternative schemes (§8.2).
2. Hyades’s pipeline-parallel aggregation design speeds up the average time of a training round by up to $2.1 \times$ (§8.3).
3. Hyades achieves a similar time-to-accuracy performance compared with the non-private counterpart. (§8.4).

8.1 Methodology

Datasets and Models. We run two image classification applications of different scales. The first dataset is CIFAR-10 [46] with 60k colored images in 10 classes. We train a ResNet-18 [35] (11M parameters) over 100 clients. We make clients’ data non-IID by applying latent Dirichlet allocation (LDA) [9, 11, 36, 66]. The concentration parameters are all set to be 1.0 such that label distributions are highly skewed across clients. The second dataset, FEMNIST [18], has 805k greyscale images in 62 classes. It is partitioned by the original data owners, and we merge every three owners’ data to form a client’s dataset. We train a CNN model [10, 42] (1M parameters) over 1000 clients.

Experiment Setup. We launch an AWS EC2 `r5.4xlarge` instance (16 vCPUs and 128 GB memory) for the server. In addition, we use one `c5.xlarge` (4 vCPUs and 8 GB memory) instance for each sampled client, aiming to match the computing power of mobile devices. To emulate hardware heterogene-

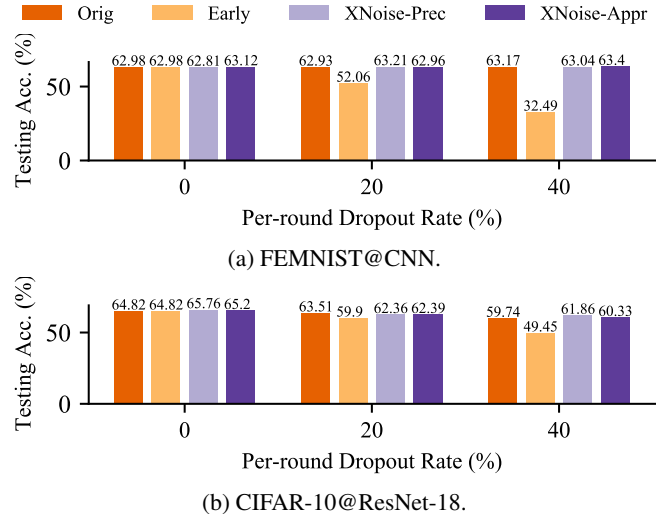


Figure 8: Final model accuracy.

ity, we introduce barriers to clients’ execution such that their response latencies follow the Zipf distribution [38, 40, 50, 76] with $a = 1.2$ (moderately skewed), i.e., the end-to-end latency of the i -th slowest client is proportional to i^{-a} . Moreover, we also emulate network heterogeneity by throttling clients’ bandwidth to fall into the range [21Mbps, 210Mbps] to match the typical mobile bandwidth [25] and meanwhile follow another independent Zipf distribution with $a = 1.2$.

Hyperparameters. As for FL training, we consistently use the mini-batch SGD with momentum set as 0.9. The number of training rounds and local epochs are 50 and 2 in FEMNIST, and 150 and 1 in CIFAR-10, respectively. Also, we set 20 and 0.01 as the batch size and learning rate in FEMNIST, while those for CIFAR-10 are 128 and 0.005, respectively.

As for distributed DP, the privacy budget ϵ is 6, and δ is the reciprocal of the total number of clients. We fix the signal bound multiplier $k = 3$, bias $\beta = e^{-0.5}$, and bit-width $b = 16$ to configure DSkellam [10]. The L2-norm clipping bounds [10] for FEMNIST and CIFAR-10 are 1 and 3, respectively. The upper bounds of sampling rate (§4) are 0.1 and 0.16, respectively; thus, up to 100 and 16 clients participate in each round for training FEMNIST and CIFAR-10, respectively.

Baselines. We compare Hyades to the following baselines:

1. **Orig:** the original, commonly-used distributed DP protocol which can neither enforce the target noise level (Definition 2 in §5) nor accelerate with pipeline execution.
2. **Early:** the same as **Orig** except that it will stop as soon as the privacy budget runs out (as mentioned in §2.3).

8.2 Effectiveness of Noise Enforcement

We first evaluate the effectiveness of Hyades’s dropout-resilient noise enforcement schemes (Xnoise-Prec and Xnoise-Appr). We vary the per-round dropout rate from 0

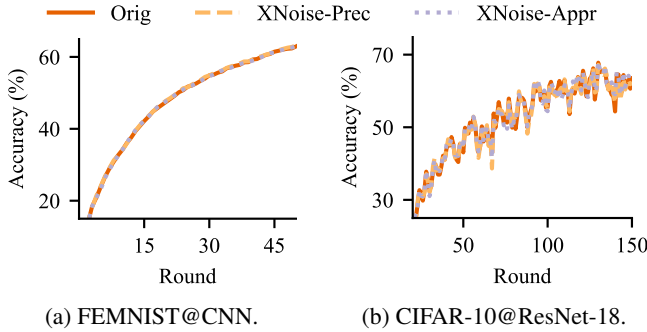


Figure 9: Round-to-accuracy performance (20% dropout). We omit `Early` as it overlaps with `Orig` while being cut at the 26-th and 114-th round in FEMNIST and CIFAR-10, respectively.

to 40% to simulate the after-sampling dropout of various severities. Note that, the before-sampling dropout has *always* been handled by our dropout-resilient privacy accounting (§4); therefore, we omit its evaluation result due to space limit.

Xnoise-Prec Improves Privacy-Utility tradeoff. Figure 7 depicts the end-to-end privacy budget consumption. As expected, both `Early` and `XNoise-Prec` consistently achieve the target privacy ($\epsilon = 6$) across all cases, either by cutting short the number of training rounds or by effectively enforcing the target aggregate noise level (Theorem 2). On the other hand, due to the missing noise contributions from dropped clients, the overall privacy budget consumed by `Orig` explosively grows when client dropout becomes more severe. For example, when the dropout rate reaches 40%, training FEMNIST and CIFAR-10 to the preset number of rounds ends up consuming an ϵ of 14.9 and 8.4, respectively.

We also compare the final model accuracy across different protocols in Figure 8. Compared to the less-private `Orig`, our `Xnoise-Prec` converges at the same speed (as shown in the learning curves in Figure 9) and induces at most 1.2% accuracy loss as it uses the minimum noise required to retain the target privacy. In contrast, despite being private, `Early` induces up to 30.5% and 15.4% accuracy loss in FEMNIST and CIFAR-10, respectively, compared to `XNoise-Prec`. This is simply because `Early` stops early due to the quick exhaustion of privacy budget. For example, when the per-round dropout rate is 20%, `Early` has to stop at Round 26 and Round 114 for FEMNIST and CIFAR-10, respectively. In summary, these baseline approaches bias towards either privacy or utility, while `XNoise-Prec` navigates the sweet point of both.

Xnoise-Appr Achieves Comparable Improvements. Figure 7 shows that the privacy budget that `Xnoise-Appr` consumes is *no* more than the target value in any case, since `Xnoise-Appr` never yields an insufficiently protected aggregate update (Theorem 3). Also, `Xnoise-Appr` induces negligible loss in final model accuracy by at most 1.1% compared to `Orig` (Figure 8). This attributes to the fact that the noise used by `Xnoise-Appr` will not exceed the minimum

necessary level by more than a factor of $O(1/n)$, where n is the number of sampled clients (Theorem 3). Note that, in some cases, `Xnoise-Appr` achieves even higher accuracy than `Xnoise-Prec`. This is because the stochasticity introduced by excessive noise can work as a regularizer to reduce overfitting. As a summary, despite trading some precision in noise enforcement, `XNoise-Appr` achieves a comparable improvement of the privacy-utility tradeoff as compared to `Xnoise-Prec`.

8.3 Efficiency of Pipeline Acceleration

We next evaluate the runtime of a training round in real deployments. To study the impact of model sizes, we additionally train a VGG-19 model [71] (20M parameters) over the CINIC-10 dataset [27]. We set the number of local epochs and batch size to 1 and 128, respectively.

Hyades Incurs Acceptable Overhead in Plain Execution without Pipelining. Figure 10 shows the average time of a training round, and breaks it into two parts: ‘agg’ that relates to distributed DP operations, and ‘other’ that relates to remaining workflow operations (e.g., model training). In a plain execution without pipeline acceleration, `Xnoise-Prec` inflates the round time by less than 27% compared to `Orig`, if 20% clients drop after being sampled; if no client drops, the overhead could become larger, varying between 16% and 49%. That said, even *without* pipeline acceleration, we believe the cost is still moderate and worth paying, as the target privacy is *always* enforced under unpredictable dropout dynamics.

As for `XNoise-Appr` that aims to trade precision for reduced asymptotic complexity during noise enforcement (§5.2), it reduces the runtime overhead of `Xnoise-Prec` by up to 25% (Figure 10). Note that, there does not exist a monotonic relationship between the speedup of `Xnoise-Appr` and the dropout severity, because the number of noise components that `Xnoise-Appr` has to remove depends only on the binary representation of the number of dropped clients (Definition 4).

Hyades Significantly Benefits from Pipelining. Figure 10 shows that our pipeline acceleration is general and can benefit all these aggregation protocols in FL. With pipelining, `Orig`, `XNoise-Prec`, and `Xnoise-Appr` can be speeded up by up to $1.1\times$ in FEMNIST, $1.6\times$ in CIFAR-10, and $2.0\times$ in CINIC-10, respectively, when no client drops out. Similarly, when 20% of clients drop out, the three protocols can all be accelerated by up to $2.1\times$. We thus make three observations. First, the execution of distributed DP can indeed be significantly expedited by utilizing idle resources (§6.1). Second, larger models can gain a more salient speedup, because their resource utilization has more potential to be improved (e.g., due to a larger degree to which the uses of different resources can be overlapped). Third, both `Xnoise-Prec` and `Xnoise-Appr` have higher efficiency gains than `Orig`.

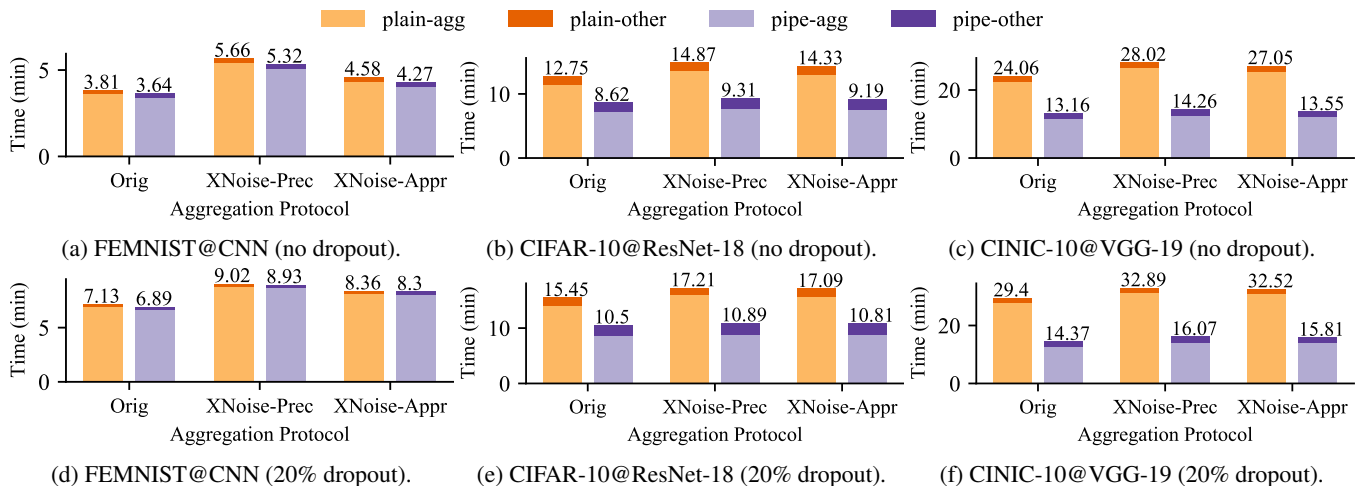


Figure 10: The breakdown of the training time of a round for **plain** execution and **pipeline** acceleration.

Table 3: End-to-end time-to-accuracy performance.

Dataset (Target Acc.)	Dropout Rate	Orig		XNoise-Prec		XNoise-Appr	
		plain	pipe	plain	pipe	plain	pipe
FEMNIST (62.8%)	0%	3.2h	3.0h	4.7h	4.4h	3.8h	3.6h
	20%	5.9h	5.7h	7.5h	7.4h	7.0h	6.9h
CIFAR-10 (67.2%)	0%	27.8h	18.8h	32.5h	20.3h	30.3h	19.4h
	20%	33.5h	22.8h	37.3h	23.6h	37.0h	23.4h

8.4 End-to-End Comparison

We finally compare the existing distributed DP solution (i.e., Orig with plain execution) against Hyades (XNoise-Prec or XNoise-Appr, with pipeline acceleration) in an end-to-end manner. We evaluate the time-to-accuracy performance, where the target FL accuracy is set to 62.8% in FEMNIST and 67.2% in CIFAR-10. These accuracy targets are set following the practice in [10] and based on the fact that our privacy target is 6. As this comparison would incur exceedingly large costs if performed in such a large-scale real deployment with 100 or even 1000 clients over a long period of time, we instead utilize the evaluation results in §8.2 and the runtime profiling results in §8.3 to project the total time taken to reach the target accuracy. As summarized in Table 3, compared to the existing solution that is non-private under client dropout, Hyades using XNoise-Prec (resp. XNoise-Appr) can always enforce the required privacy, while achieving the target accuracy with moderately higher training time of 25–38% (resp. 13–17%) in FEMNIST or even shortening it by 27–30% (resp. consistently 30%) in CIFAR-10. To conclude, Hyades pursues privacy at a low or even no expense of training efficiency.

9 Discussion and Future Work

Handling Mild Collusion. Hyades can be easily extended to a scenario where the server colludes with a small number of clients (i.e., mild collusion). This is reasonable as, in reality, the number of clients is large, and the chance of having a colluded client sampled by the server is small² (e.g., tens to hundreds of clients sampled from millions of devices [16, 44]). Knowing that only a small fraction of participants (e.g., <1%) can collude, clients can add slightly more noises to their updates to tolerate it, with little impact on the model utility.

Secure Client Sampling. Existing secure aggregation protocols require clients to be indexable, so that clients can perform pairwise masking in SecAgg. On the other hand, privacy amplification via subsampling requires that the sampling outcomes are concealed from the adversary. To meet both requirements, one can use virtual client indexes that are refreshed every round and make them unlinkable to the actual client identities. This can be achieved with mix networks [21, 47], which we leave for future work.

10 Related Work

DP-FedAvg [54, 65] is the first DP-protected FL system that uses central DP. Assuming the same threat model, Distributed DP-SGD [13] and DP-FTRL [43] identify the technical challenge brought by uniform client sampling but sidestep it with alternative methods for privacy amplification. Unlike such work, Hyades does not assume a trusted server.

Existing studies that use distributed DP in FL focus on secure aggregation and DP algorithm design. Notably, DDGauss [42] and DSkellam [10] carefully combine the DP noise addition with SecAgg for end-to-end privacy analysis.

²An honest-but-curious server does not intentionally sample colluded clients since it needs to follow the sampling algorithm faithfully.

FLDP [75] explores aggregation based on the learning with errors (LWE) problem [67], in which the residual errors are used as DP noise. Hyades complements these studies with dropout resilience and improved execution efficiency.

11 Conclusion

Distributed differential privacy (DP) has long been appealing to federated learning (FL) as it achieves an informed privacy-utility tradeoff without a trusted server. This paper presents Hyades, an efficient FL framework that enables dropout-resilient distributed DP in realistic FL scenarios. To handle client dropout before sampling, Hyades develops a new analytical tool for privacy accounting, and uses it to determine the minimum required noise in each training round. Hyades then designs a novel add-then-remove scheme to enforce the required noise at exactly the target level, regardless of client dropout after being sampled. Hyades also enables pipeline parallelism for accelerated secure aggregation with an efficient pipeline execution scheme. Compared to the existing distributed DP mechanisms, Hyades efficiently achieves the highest training accuracy without compromising privacy guarantees in the presence of client dropout.

References

- [1] Cryptography. <https://cryptography.io/>.
- [2] Google research. <https://github.com/google-research/google-research>.
- [3] Nginx: Advanced load balancer, web server, and reverse proxy. <https://www.nginx.com/>.
- [4] Pycryptodome. <https://www.pycryptodome.org/>.
- [5] Python socket.io server and client. <https://github.com/miguelgrinberg/python-socketio>.
- [6] Redis in-memory data structure store. <https://redis.io/>.
- [7] Tensorflow privacy. <https://github.com/tensorflow/privacy>.
- [8] Martin Abadi, Andy Chu, Ian Goodfellow, H Brendan McMahan, Ilya Mironov, Kunal Talwar, and Li Zhang. Deep learning with differential privacy. In *CCS*, 2016.
- [9] Durmus Alp Emre Acar, Yue Zhao, Ramon Matas Navarro, Matthew Mattina, Paul N Whatmough, and Venkatesh Saligrama. Federated learning based on dynamic regularization. In *ICLR*, 2021.
- [10] Naman Agarwal, Peter Kairouz, and Ziyu Liu. The Skellam mechanism for differentially private federated learning. In *NeurIPS*, 2021.
- [11] Maruan Al-Shedivat, Jennifer Gillenwater, Eric Xing, and Afshin Rostamizadeh. Federated learning via posterior averaging: A new perspective and practical algorithms. In *ICLR*, 2020.
- [12] Arm. Trustzone technology. <https://developer.arm.com/ip-products/security-ip/trustzone>, 2021.
- [13] Borja Balle, Peter Kairouz, Brendan McMahan, Om Thakkar, and Abhradeep Guha Thakurta. Privacy amplification via random check-ins. In *NeurIPS*, 2020.
- [14] James Henry Bell, Kallista A Bonawitz, Adrià Gascón, Tancrède Lepoint, and Mariana Raykova. Secure single-server aggregation with (poly) logarithmic overhead. In *CCS*, 2020.
- [15] Andrea Bittau, Úlfar Erlingsson, Petros Maniatis, Ilya Mironov, Ananth Raghunathan, David Lie, Mitch Rudominer, Ushasree Kode, Julien Tinnes, and Bernhard Seefeld. Prochlo: Strong privacy for analytics in the crowd. In *SOSP*, 2017.
- [16] Keith Bonawitz, Hubert Eichner, Wolfgang Grieskamp, Dzmitry Huba, Alex Ingerman, Vladimir Ivanov, Chloe Kiddon, Jakub Konečný, Stefano Mazzocchi, Brendan McMahan, et al. Towards federated learning at scale: System design. In *MLSys*, 2019.
- [17] Keith Bonawitz, Vladimir Ivanov, Ben Kreuter, Antonio Marcedone, H Brendan McMahan, Sarvar Patel, Daniel Ramage, Aaron Segal, and Karn Seth. Practical secure aggregation for privacy-preserving machine learning. In *CCS*, 2017.
- [18] Sebastian Caldas, Sai Meher Karthik Duddu, Peter Wu, Tian Li, Jakub Konečný, H Brendan McMahan, Virginia Smith, and Ameet Talwalkar. Leaf: A benchmark for federated settings. In *NeurIPS Workshop*, 2019.
- [19] Nicholas Carlini, Chang Liu, Úlfar Erlingsson, Jernej Kos, and Dawn Song. The secret sharer: Evaluating and testing unintended memorization in neural networks. In *USENIX Security*, 2019.
- [20] Zheng Chai, Ahsan Ali, Syed Zawad, Stacey Truex, Ali Anwar, Nathalie Baracaldo, Yi Zhou, Heiko Ludwig, Feng Yan, and Yue Cheng. Tifl: A tier-based federated learning system. In *HPDC*, 2020.
- [21] David L Chaum. Untraceable electronic mail, return addresses, and digital pseudonyms. *Communications of the ACM*, 24(2):84–90, 1981.
- [22] Zitai Chen, Georgios Vasilakis, Kit Murdock, Edward Dean, David Oswald, and Flavio D Garcia. Voltpillager: Hardware-based fault injection attacks against intel sgx

- enclaves using the svid voltage scaling interface. In *USENIX Security*, 2021.
- [23] Albert Cheu, Adam Smith, Jonathan Ullman, David Zerber, and Maxim Zhilyaev. Distributed differential privacy via shuffling. In *Eurocrypt*, 2019.
- [24] Beongjun Choi, Jy-yong Sohn, Dong-Jun Han, and Jaekyun Moon. Communication-computation efficient secure aggregation for federated learning. *arXiv:2012.05433*, 2020.
- [25] Cisco. Cisco annual internet report (2018–2023) white paper, 2020. <https://support.google.com/messages/answer/9327902>.
- [26] Dwork Cynthia. Differential privacy. *Automata, languages and programming*, pages 1–12, 2006.
- [27] Luke N Darlow, Elliot J Crowley, Antreas Antoniou, and Amos J Storkey. Cinic-10 is not imagenet or cifar-10. *arXiv:1810.03505*, 2018.
- [28] Jieren Deng, Yijue Wang, Ji Li, Chenghong Wang, Chao Shang, Hang Liu, Sanguthevar Rajasekaran, and Caiwen Ding. Tag: Gradient attack on transformer-based language models. In *EMNLP*, 2021.
- [29] Dimitar I Dimitrov, Mislav Balunović, Nikola Jovanović, and Martin Vechev. Lamp: Extracting text from gradients with language model priors. *arXiv:2202.08827*, 2022.
- [30] Cynthia Dwork, Frank McSherry, Kobbi Nissim, and Adam Smith. Calibrating noise to sensitivity in private data analysis. In *Theory of cryptography conference*, pages 265–284. Springer, 2006.
- [31] Cynthia Dwork and Aaron Roth. The algorithmic foundations of differential privacy. *Foundations and Trends in Theoretical Computer Science*, 9(3–4):211–407, 2014.
- [32] Úlfar Erlingsson, Vitaly Feldman, Ilya Mironov, Ananth Raghunathan, Kunal Talwar, and Abhradeep Thakurta. Amplification by shuffling: From local to central differential privacy via anonymity. In *SODA*, 2019.
- [33] Google. Your chats stay private while messages improves suggestions, 2021. <https://support.google.com/messages/answer/9327902>.
- [34] Samyak Gupta, Yangsibo Huang, Zexuan Zhong, Tianyu Gao, Kai Li, and Danqi Chen. Recovering private text in federated learning of language models. *arXiv:2205.08514*, 2022.
- [35] Kaiming He, Xiangyu Zhang, Shaoqing Ren, and Jian Sun. Deep residual learning for image recognition. In *CVPR*, 2016.
- [36] Tzu-Ming Harry Hsu, Hang Qi, and Matthew Brown. Measuring the effects of non-identical data distribution for federated visual classification. *arXiv:1909.06335*, 2019.
- [37] Intel. Software guard extensions. <https://software.intel.com/content/www/us/en/develop/topics/software-guard-extensions.html>, 2021.
- [38] Zhipeng Jia and Emmett Witchel. Boki: Stateful serverless computing with shared logs. In *SOSP*, 2021.
- [39] Zhifeng Jiang, Wei Wang, Baochun Li, and Bo Li. Pisces: Efficient federated learning via guided asynchronous training. In *SoCC*, 2022.
- [40] Zhifeng Jiang, Wei Wang, Bo Li, and Qiang Yang. Towards efficient synchronous federated training: A survey on system optimization strategies. *IEEE Transactions on Big Data*, 2022.
- [41] Swanand Kadhe, Nived Rajaraman, O Ozan Koyluoglu, and Kannan Ramchandran. Fastsecagg: Scalable secure aggregation for privacy-preserving federated learning. *arXiv:2009.11248*, 2020.
- [42] Peter Kairouz, Ziyu Liu, and Thomas Steinke. The distributed discrete gaussian mechanism for federated learning with secure aggregation. In *ICML*, 2021.
- [43] Peter Kairouz, Brendan McMahan, Shuang Song, Om Thakkar, Abhradeep Thakurta, and Zheng Xu. Practical and private (deep) learning without sampling or shuffling. In *ICML*, 2021.
- [44] Peter Kairouz, H Brendan McMahan, Brendan Avent, Aurélien Bellet, Mehdi Bennis, Arjun Nitin Bhagoji, Keith Bonawitz, Zachary Charles, Graham Cormode, Rachel Cummings, et al. Advances and open problems in federated learning. *Foundations and Trends in Machine Learning*, 14(1), 2021.
- [45] Young Geun Kim and Carole-Jean Wu. Autofl: Enabling heterogeneity-aware energy efficient federated learning. In *MICRO*, 2021.
- [46] Alex Krizhevsky, Geoffrey Hinton, et al. Learning multiple layers of features from tiny images. 2009.
- [47] Albert Kwon, David Lazar, Srinivas Devadas, and Bryan Ford. Riffle. In *PETS*, 2016.
- [48] Fan Lai, Yinwei Dai, Sanjay S Singapuram, Jiachen Liu, Xiangfeng Zhu, Harsha V Madhyastha, and Mosharaf Chowdhury. FedScale: Benchmarking model and system

- performance of federated learning at scale. In *ICML*, 2022.
- [49] Fan Lai, Xiangfeng Zhu, Harsha V. Madhyastha, and Mosharaf Chowdhury. Oort: Efficient federated learning via guided participant selection. In *OSDI*, 2021.
- [50] Yunseong Lee, Alberto Scolari, Byung-Gon Chun, Marco Domenico Santambrogio, Markus Weimer, and Matteo Interlandi. Pretzel: Opening the black box of machine learning prediction serving systems. In *OSDI*, 2018.
- [51] Wenqi Li, Fausto Milletari, Daguang Xu, Nicola Rieke, Jonny Hancox, Wentao Zhu, Maximilian Baust, Yan Cheng, Sébastien Ourselin, M Jorge Cardoso, et al. Privacy-preserving federated brain tumour segmentation. In *MLMI Workshop*, 2019.
- [52] Heiko Ludwig, Nathalie Baracaldo, Gegi Thomas, Yi Zhou, Ali Anwar, Shashank Rajamoni, Yuya Ong, Jayaram Radhakrishnan, Ashish Verma, Mathieu Sinn, et al. Ibm federated learning: an enterprise framework white paper v0.1. *arXiv:2007.10987*, 2020.
- [53] Brendan McMahan, Eider Moore, Daniel Ramage, Seth Hampson, and Blaise Aguera y Arcas. Communication-efficient learning of deep networks from decentralized data. In *AISTATS*, 2017.
- [54] H Brendan McMahan, Daniel Ramage, Kunal Talwar, and Li Zhang. Learning differentially private recurrent language models. In *ICLR*, 2018.
- [55] Luca Melis, Congzheng Song, Emiliano De Cristofaro, and Vitaly Shmatikov. Exploiting unintended feature leakage in collaborative learning. In *IEEE S&P*, 2019.
- [56] Ralph C Merkle. Secure communications over insecure channels. *Communications of the ACM*, 21(4):294–299, 1978.
- [57] Ilya Mironov. Rényi differential privacy. In *2017 IEEE 30th computer security foundations symposium (CSF)*, pages 263–275. IEEE, 2017.
- [58] Milad Nasr, Reza Shokri, and Amir Houmansadr. Comprehensive privacy analysis of deep learning: Passive and active white-box inference attacks against centralized and federated learning. In *IEEE S&P*, 2019.
- [59] NVIDIA. Triaging covid-19 patients: 20 hospitals in 20 days build ai model that predicts oxygen needs, 2020. <https://blogs.nvidia.com/blog/2020/10/05/federated-learning-covid-oxygen-needs/>.
- [60] Adam Paszke, Sam Gross, Francisco Massa, Adam Lerer, James Bradbury, Gregory Chanan, Trevor Killeen, Zeming Lin, Natalia Gimelshein, Luca Antiga, et al. Pytorch: An imperative style, high-performance deep learning library. In *NeurIPS*, 2019.
- [61] Matthias Paulik, Matt Seigel, Henry Mason, Dominic Telaar, Joris Kluivers, Rogier van Dalen, Chi Wai Lau, Luke Carlson, Filip Granqvist, Chris Vandeveld, et al. Federated evaluation and tuning for on-device personalization: System design & applications. *arXiv:2102.08503*, 2021.
- [62] Le Trieu Phong, Yoshinori Aono, Takuya Hayashi, Lihua Wang, and Shiho Moriai. Privacy-preserving deep learning via additively homomorphic encryption. *IEEE Transactions on Information Forensics and Security*, 13(5):1333–1345, 2018.
- [63] Vasyli Pihur, Aleksandra Korolova, Frederick Liu, Subhash Sankuratripati, Moti Yung, Dachuan Huang, and Ruogu Zeng. "Differentially-private" draw and discard" machine learning. *arXiv:1807.04369*, 2018.
- [64] Aurick Qiao, Bryon Aragam, Bingjing Zhang, and Eric Xing. Fault tolerance in iterative-convergent machine learning. In *ICML*, 2019.
- [65] Swaroop Ramaswamy, Om Thakkar, Rajiv Mathews, Galen Andrew, H Brendan McMahan, and Françoise Beaufays. Training production language models without memorizing user data. *arXiv:2009.10031*, 2020.
- [66] Sashank J Reddi, Zachary Charles, Manzil Zaheer, Zachary Garrett, Keith Rush, Jakub Konečný, Sanjiv Kumar, and Hugh Brendan McMahan. Adaptive federated optimization. In *ICLR*, 2020.
- [67] Oded Regev. On lattices, learning with errors, random linear codes, and cryptography. *Journal of the ACM*, 56(6):1–40, 2009.
- [68] Aaron Roth. The algorithmic foundations of data privacy. <https://www.cis.upenn.edu/~aaroth/courses/slides/Lecture4.pdf>, 2011.
- [69] Adi Shamir. How to share a secret. *Communications of the ACM*, 22(11):612–613, 1979.
- [70] Reza Shokri, Marco Stronati, Congzheng Song, and Vitaly Shmatikov. Membership inference attacks against machine learning models. In *IEEE S&P*, 2017.
- [71] Karen Simonyan and Andrew Zisserman. Very deep convolutional networks for large-scale image recognition. *arXiv:1409.1556*, 2014.
- [72] Jinhyun So, Başak Güler, and A Salman Avestimehr. Turbo-aggregate: Breaking the quadratic aggregation barrier in secure federated learning. *IEEE Journal on*

Selected Areas in Information Theory, 2(1):479–489, 2021.

- [73] Jinhyun So, Corey J Nolet, Chien-Sheng Yang, Songze Li, Qian Yu, Ramy E Ali, Basak Guler, and Salman Avestimehr. Lightsecagg: a lightweight and versatile design for secure aggregation in federated learning. In *MLSys*, 2022.
- [74] Congzheng Song and Vitaly Shmatikov. Auditing data provenance in text-generation models. In *SIGKDD*, 2019.
- [75] Timothy Stevens, Christian Skalka, Christelle Vincent, John Ring, Samuel Clark, and Joseph Near. Efficient differentially private secure aggregation for federated learning via hardness of learning with errors. In *USENIX Security*, 2022.
- [76] Huangshi Tian, Minchen Yu, and Wei Wang. Crystalperf: Learning to characterize the performance of dataflow computation through code analysis. In *ATC*, 2021.
- [77] Jo Van Bulck, Marina Minkin, Ofir Weisse, Daniel Genkin, Baris Kasikci, Frank Piessens, Mark Silberstein, Thomas F Wenisch, Yuval Yarom, and Raoul Strackx. Foreshadow: Extracting the keys to the intel sgx kingdom with transient out-of-order execution. In *USENIX Security*, 2018.
- [78] Yu-Xiang Wang, Borja Balle, and Shiva Prasad Kasiviswanathan. Subsampled Rényi differential privacy and analytical moments accountant. In *AISTATS*, 2019.
- [79] Zhibo Wang, Mengkai Song, Zhifei Zhang, Yang Song, Qian Wang, and Hairong Qi. Beyond inferring class representatives: User-level privacy leakage from federated learning. In *INFOCOM*, 2019.
- [80] WeBank. Utilization of fate in anti money laundering through multiple banks, 2020. <https://www.fedai.org/cases/utilization-of-fate-in-anti-money-laundering-through-multiple-banks/>.
- [81] Chengxu Yang, Qipeng Wang, Mengwei Xu, Zhenpeng Chen, Kaigui Bian, Yunxin Liu, and Xuanzhe Liu. Characterizing impacts of heterogeneity in federated learning upon large-scale smartphone data. In *WWW*, 2021.
- [82] Jiayuan Ye, Aadyaa Maddi, Sasi Kumar Murakonda, and Reza Shokri. Enhanced membership inference attacks against machine learning models. In *CCS*, 2022.
- [83] Ligeng Zhu, Zhijian Liu, and Song Han. Deep leakage from gradients. In *NeurIPS*, 2019.
- [84] Yuqing Zhu and Yu-Xiang Wang. Poission subsampled Rényi differential privacy. In *ICML*, 2019.

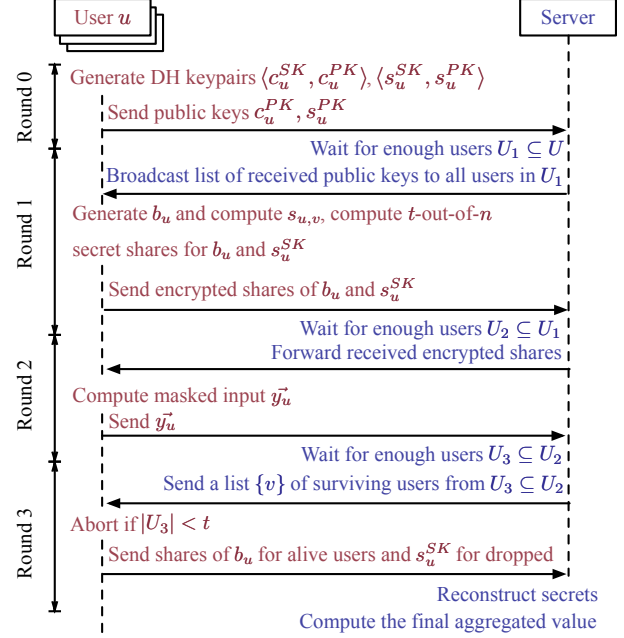


Figure 11: SecAgg’s protocol in the semi-honest threat model [17].

A The SecAgg protocol

Technical Details. Here we provide a detailed description of how SecAgg [17] works under the semi-honest adversary. As depicted in Fig. 11, the protocol consists of four communication rounds.

- *Round 0 (Advertise Keys):* each client $u \in U$ generates key pairs $\langle c_u^{SK}, c_u^{PK} \rangle, \langle s_u^{SK}, s_u^{PK} \rangle$ and sends (c_u^{PK}, s_u^{PK}) to all of her neighbors with the relaying help of the server.
- *Round 1 (Share Keys):* each of the alive clients $u \in U_1 \subseteq U$ runs the Diffie-Hellman key agreement protocol [56] that derives a shared random key $s_{u,v} = \mathcal{KA}.Agree(s_u^{SK}, s_v^{PK})$ for every other client $v \in U_1$.³ Client u also randomly samples a seed b_u , and securely shares s_u^{SK} and b_u to each of the other client v ’s by sending it the respective t -out-of- n shares encrypted using the corresponding agreed key $\mathcal{KA}.Agree(c_u^{SK}, c_v^{PK})$ ’s.
- *Round 2 (Masked Input Collection):* each surviving client $u \in U_2$ prepares a pairwise mask $\vec{m}_{u,v} = PRG(s_{u,v})$ derived from shared keys with each of the other client v ’s. She also generates a self mask $\vec{r}_u = PRG(b_u)$, masks her vector input \vec{x}_u in the following manner and then sends the masked input \vec{y}_u to the server:

$$\vec{y}_u = \vec{x}_u + \vec{r}_u - \sum_{v < u, v \in U_2} \vec{m}_{u,v} + \sum_{v > u, v \in U_2} \vec{m}_{u,v}. \quad (6)$$

³Note that $\mathcal{KA}.Agree(\cdot, \cdot)$ is symmetric and thus $s_{u,v} = s_{v,u}$

- *Round 3 (Unmasking)*: summing up masked inputs submitted by surviving clients U_3 , the server obtains:

$$\sum_{u \in U_3} \vec{x}_u + \underbrace{\sum_{u \in U_3} \vec{r}_u}_A + \underbrace{\sum_{u \in U_2/U_3} \left(\sum_{v < u, v \in U_3} \vec{m}_{u,v} - \sum_{v > u, v \in U_3} \vec{m}_{u,v} \right)}_B. \quad (7)$$

Then, to remove part A , for each surviving client $u \in U_3$, the server compute \vec{r}_u by reconstructing b_u with over t shares of it collected from surviving clients U_4 . Similarly, to remove part B , for each dropped clients $u \in U_2/U_3$, the server reconstructs its secret key c_u^{SK} by collecting over t shares of it from U_4 . Together with the public keys of v 's from $U_2/\{u\}$ to reconstruct $s_{u,v}$'s, the server finally computes and removes all the related $\vec{m}_{u,v}$'s.

Source of Complexity. We now pinpoint two main sources of SecAgg's inefficiency (§2.3). The first source is the use of Shamir's t -out-of- n secret sharing scheme [69] (Round 1). It is employed to gain resilience against client dropout, as it allows a secret to be split and shared to n clients so that any t clients can provide enough information to reconstruct it. For a client, generating Shamir's t -out-of- n secret takes $O(n^2)$ time, yielding a quadratic computation overhead w.r.t. the number of sampled clients ($O(|U_1|^2)$). The second source is the design of *pairwise masking*, where each client adds a pairwise mask (of the same length d as the model) to her update for each of the other alive clients (Round 2), and the server needs to unmask these masks for each dropped client (Round 3). This helps tolerate colluding parties, as the pairwise masks between any two benign clients will be concealed from the adversary. However, it induces quadratic computation overhead to both clients ($O(d|U_2|^2)$) and the server ($O(d|U_3|^2)$).

B Rényi DP

Here we provide a detailed primer on Rényi DP [57] to help the reader better understand the few facts introduced in §4.

Rényi Divergence. The Rényi divergence of order $\alpha \in (1, \infty)$ between two distributions P and Q defined over R , noted $D_\alpha(P \parallel Q)$, is defined as:

$$D_\alpha(P \parallel Q) \triangleq \frac{1}{\alpha - 1} \log \mathbb{E}_{x \sim Q} \left(\frac{P(x)}{Q(x)} \right)^\alpha, \quad (8)$$

where all logarithms are natural and $P(x)$ is the density of P at x . It can be verified that there is a relationship between the Rényi divergence with $\alpha = \infty$ and $(\epsilon, 0)$ -differential privacy. Specifically, by definition,

$$D_\infty(f(D) \parallel f(D')) = \sup_{x \in \text{supp } f(D')} \log \frac{f(D)}{f(D')}. \quad (9)$$

On the other hand, as mentioned in §4, $(\epsilon, 0)$ -DP is defined by putting a multiplicative bound on the change in the output distribution: $\forall R, \log \frac{\Pr[f(D) \in R]}{\Pr[f(D') \in R]} \leq \epsilon$. Combining the above two facts, we know that a randomized mechanism f is $(\epsilon, 0)$ -differentially private if and only if its distribution over any two adjacent inputs D and D' satisfies $D_\infty(f(D) \parallel f(D')) \leq \epsilon$. To relax $(\epsilon, 0)$ -differential privacy based on the order α used in the Rényi divergence, Rényi DP is invented as introduced next.

Definition and Translation to Traditional DP. Formally, a randomized algorithm f is (α, ϵ) -Rényi DP if:

$$D_\alpha(f(D) \parallel f(D')) \leq \epsilon. \quad (10)$$

Thus, as derived above, (∞, ϵ) -Rényi DP is equivalent to $(\epsilon, 0)$ -DP. Furthermore, there is also a clear formula to translate (α, ϵ) -Rényi DP into (ϵ, δ) -DP:

Theorem 4. (Proposition 3 in [57]) *If f is an (α, ϵ) -Rényi DP mechanism, it also satisfies $(\epsilon + \frac{\log 1/\delta}{\alpha - 1}, \delta)$ -differential privacy for any $0 < \delta < 1$.*

As the formula holds for all $\alpha > 1$, one can choose the α that yields the best DP guarantee (i.e., the smallest ϵ when δ is fixed) when translating Rényi DP to DP.

Strong Composition. Unlike (ϵ, δ) -DP where the privacy guarantee is expressed with mechanism-agnostic parameters, Rényi DP accounts for the specifically used randomized mechanism in that its ϵ is typically given as a mechanism-specific function of α , i.e., $\epsilon(\alpha)$. Thus, when composing a sequence of (heterogeneous) mechanisms, analysis with Rényi DP often yields a tighter privacy loss compared to that with (ϵ, δ) -DP. For instance, an Rényi DP composition of k Gaussian mechanisms each with noise level σ^2 (i.e., the variance) yields a privacy loss identical to that of a Gaussian mechanism with noise level σ/k , instead of σ/k^2 as with basic composition theory in (ϵ, δ) -DP.

C Proofs for Privacy Accounting Results

Proof for Theorem 1 (§4).

Proof. We follow the notation used in Theorem 1. We assume $C' = C \cup \{c\}$ for some client c and the rest of clients C . We denote by q the density of $g(C')$ and p the density of $g(C)$. In order to bound RDP with order α , it requires to bound the moments $\mathbb{E}_p[(q/p)^\alpha]$ and $\mathbb{E}_q[(p/q)^\alpha]$ at the same time for each c . We start the proof with a few intuitions.

1. Suppose that $|C| = n - 1$ (and thus $|C'| = n$). By conditioning on the inclusion of all clients but c , i.e., conditioning on $J = (\xi_1, \dots, \xi_{n-1}) \in \{0, 1\}^{n-1}$, we can rewrite the two moments as

$$\mathbb{E}_p[(q/p)^\alpha] = \int \frac{(\mathbb{E}_J[(1-\gamma)\mu_0(J) + \gamma\mu_1(J)])^\alpha}{(\mathbb{E}_J[\mu_0(J)])^{\alpha-1}},$$

$$\mathbb{E}_q[(p/q)^\alpha] = \int \frac{(\mathbb{E}_J[\mu_0(J)])^\alpha}{(\mathbb{E}_J[(1-\gamma)\mu_0(J) + \gamma\mu_1(J)])^{\alpha-1}},$$

where $\mu_0(J)$ is the distribution of $f(C_J)$, $\mu_1(J)$ is the distribution of $f(C_J \cup \{c\})$, and $C_J = \{c_i \mid \xi_i = 1, \xi_i \in J\}$.

- When $\gamma_i = \gamma$ for all $i \in [n]$, it degenerates to the case as discussed in Theorem 5 of [84] which proves a bound for both $\mathbb{E}_p[(q/p)^\alpha]$ and $\mathbb{E}_q[(p/q)^\alpha]$ that is in the same form as what Theorem 1 aims to give. The key to proving that theorem lies in the use of the following two inequalities:

$$\mathbb{E}_p[(q/p)^\alpha] \leq \sum_J \mathbb{P}(J) \mathbb{E}_{\mu_0(J)} \left(\frac{(1-\gamma)\mu_0(J) + \gamma\mu_1(J)}{\mu_0(J)} \right)^\alpha, \quad (11)$$

$$\mathbb{E}_q[(p/q)^\alpha] \leq \sum_J \mathbb{P}(J) \mathbb{E}_{(1-\gamma)\mu_0(J) + \gamma\mu_1(J)} \left(\frac{\mu_0(J)}{(1-\gamma)\mu_0(J) + \gamma\mu_1(J)} \right)^\alpha. \quad (12)$$

For ease of use, we denote the right-hand side of the two inequalities as a $F_1(\gamma)$ and $F_2(\gamma)$, respectively.

- To prove the same bound for our studied case, it suffices to prove that both Inequality 11 and 12 still hold. Consider a particular client c whose probability of being sampled is $\gamma_i \in [0, \gamma]$. By the above mentioned existing results, we already have that $\mathbb{E}_p[(q/p)^\alpha] \leq F_1(\gamma_i)$ as well as $\mathbb{E}_q[(p/q)^\alpha] \leq F_2(\gamma_i)$, no matter what other clients' sampling probabilities are. Thus, the key of our proof is to show that $F_1(\gamma_i) \leq F_1(\gamma)$ and $F_2(\gamma_i) \leq F_2(\gamma)$ at all time. To that end, we attempt to prove that both $F_1(\gamma)$ and $F_2(\gamma)$ monotonically decrease in $\gamma \in [0, 1]$.

We start with $F_1(\gamma)$. By taking its first- and second-order derivatives.

$$F_1'(\gamma) = \alpha \sum_J \mathbb{P}(J) \mathbb{E}_{\mu_0(J)} \left[\frac{((1-\gamma)\mu_0(J) + \gamma\mu_1(J))^{\alpha-1}}{(\mu_0(J))^\alpha} (\mu_1(J) - \mu_0(J)) \right], \quad (13)$$

$$F_1''(\gamma) = \alpha(\alpha-1) \sum_J \mathbb{P}(J) \mathbb{E}_{\mu_0(J)} \left[\frac{((1-\gamma)\mu_0(J) + \gamma\mu_1(J))^{\alpha-2}}{(\mu_0(J))^\alpha} (\mu_1(J) - \mu_0(J))^2 \right]. \quad (14)$$

As $F_1''(\gamma)$ is non-negative, $F_1'(\gamma)$ is monotonically increasing in γ . Furthermore, we have that

$$\begin{aligned} F_1'(0) &= \alpha \sum_J \mathbb{P}(J) \mathbb{E}_{\mu_0(J)} \left[\frac{\mu_1(J) - \mu_0(J)}{\mu_0(J)} \right] \\ &= \alpha \sum_J \mathbb{P}(J) \int \frac{\mu_1(J) - \mu_0(J)}{\mu_0(J)} \mu_0(J) \\ &= \alpha \sum_J \mathbb{P}(J) \left(\int \mu_1(J) - \int \mu_0(J) \right) \\ &= \alpha \sum_J \mathbb{P}(J) (1 - 1) = 0. \end{aligned} \quad (15)$$

Thus, $F_1'(\gamma) \geq 0$, which implies that $F_1(\gamma)$ is monotonically increasing in γ . Similarly, we can also see that $F_2(\gamma)$ is monotonically increasing in γ , as

$$\begin{aligned} F_2'(0) &= (1-\alpha) \sum_J \mathbb{P}(J) \mathbb{E}_{(1-\gamma)\mu_0(J) + \gamma\mu_1(J)} \left[\frac{(\mu_0(J))^\alpha}{((1-\gamma)\mu_0(J) + \gamma\mu_1(J))^{\alpha-1}} \right. \\ &\quad \left. (\mu_1(J) - \mu_0(J)) \right] \Big|_{\gamma=0} = (1-\alpha) \sum_J \mathbb{P}(J) \int (\mu_1(J) - \mu_0(J)) = 0, \end{aligned} \quad (16)$$

$$\begin{aligned} F_2''(\gamma) &= \alpha(\alpha-1) \sum_J \mathbb{P}(J) \mathbb{E}_{\mu_0(J)} \left[\frac{(\mu_0(J))^\alpha}{((1-\gamma)\mu_0(J) + \gamma\mu_1(J))^\alpha} (\mu_1(J) - \mu_0(J))^2 \right] \geq 0. \end{aligned} \quad (17)$$

Now we are ready to reuse the proof of Theorem 5 in [84] (which we omit here for brevity), and finally, obtain exactly the same RDP bound for any integer $\alpha \geq 2$. \square

D Noise Enforcement Complexity Analysis

We first evaluate the complexity of XNoise-Prec (§5.1). All calculations below assume a single server and $|S|$ users, where $|D| = O(|S|)$ clients drop out after being sampled. We also use d to denote the number of parameters in a model. We ignore the cost of the used public key infrastructure but stress that including its cost does not change any of the asymptotics.

For a sampled client, its computational cost stems from (1) generating noise components, which is $O(|S|)$, (2) adding the noise components to its update, which is $O(d|S|)$ where d is the model size, measured by the number of model parameters, and (3) creating secret shares for the used PRG seeds, which is $O(|S|^3)$. Together, the computational complexity is $O(d|S| + |S|^3)$. Concerning the communication cost, it stems from (1) uploading the needed seeds for noise removal, which is $O(|S|)$, and, if necessary, (2) uploading the secret shares for recovering the other clients' missing seeds, which is $O(|S|^2)$. The overall communication complexity is hence $O(|S|^2)$.

For the server, its computational cost stems from (1) recovering the missing seeds, if any, using the optimized reconstruction technique given in [17], which is $O(|S|^3)$, and (2) generating excessive noise components using the PRG seeds and removing them, which is $O(d|S|^2)$. Thus, the overall computational complexity is $O(|S|^3 + d|S|^2)$. As for the server's communication cost, it stems from (1) receiving PRG seeds from surviving clients, which is $O(|S|^2)$, and (2) receiving secret shares for recovering the missing seeds (if any), which is $O(|S|^3)$. Overall, the communication complexity is $O(|S|^3)$.

The analysis of XNoise-Appr (§5.2) is almost the same as the above, except that each client generates $O(\log|S|)$ noise components instead of $O(|S|)$. We thus omit it for brevity.

E Proofs for Noise Enforcement Results

Proof for Theorem 2 (§5.1).

Proof. Before the server performs noise deduction, the aggregated update is randomized with noise level:

$$\begin{aligned} & \sum_{c_j \in \mathcal{S} \setminus D} \left(\frac{\sigma_*^2}{|S|} + \sum_{k=1}^t \frac{\sigma_*^2}{(|S|-k+1)(|S|-k)} \right) \\ &= \sum_{c_j \in \mathcal{S} \setminus D} \left(\frac{\sigma_*^2}{|S|} + \sum_{k=1}^t \left(\frac{\sigma_*^2}{|S|-k} - \frac{\sigma_*^2}{|S|-k+1} \right) \right) \\ &= \sigma_*^2 (|S| - |D|) \left(\frac{1}{|S|} + \frac{1}{|S|-t} - \frac{1}{|S|} \right) = \sigma_*^2 \frac{|S| - |D|}{|S| - t}. \end{aligned}$$

Moreover, the total noise level deducted by the server is:

$$\begin{aligned} & \sum_{c_j \in \mathcal{S} \setminus D} \sum_{k=|D|+1}^t \frac{\sigma_*^2}{(|S|-k+1)(|S|-k)} \\ &= (|S| - |D|) \sigma_*^2 \sum_{k=|D|+1}^t \left(\frac{1}{|S|-k} - \frac{1}{|S|-k+1} \right). \\ &= (|S| - |D|) \sigma_*^2 \left(\frac{1}{|S|-t} - \frac{1}{|S|-|D|} \right) = \sigma_*^2 \frac{t - |D|}{|S| - t}. \end{aligned}$$

Thus, the remaining noise level at the aggregated update is $\sigma_*^2 \frac{|S| - |D|}{|S| - t} - \sigma_*^2 \frac{t - |D|}{|S| - t} = \sigma_*^2$. \square

Proof for Theorem 3 (§5.2).

Proof. Before the server performs noise deduction, the aggregated update is randomized with noise level:

$$\begin{aligned} & \sum_{c_j \in \mathcal{S} \setminus D} \left(\frac{\sigma_*^2}{|S|} + \eta + \sum_{k=2}^{\tau+1} \eta \cdot 2^{k-2} \right) \\ &= \sum_{c_j \in \mathcal{S} \setminus D} \left(\frac{\sigma_*^2}{|S|} + 2^\tau \eta \right) \\ &= (|S| - |D|) \left(\frac{\sigma_*^2}{|S|} + 2^\tau \frac{\sigma_*^2 t}{2^\tau |S| (|S| - t)} \right) = \sigma_*^2 \frac{|S| - |D|}{|S| - t}. \end{aligned}$$

As for noise deduction by the server, we discuss two cases.

Case 1: First, if there is no client dropping ($|D| = 0$), the total noise level that can be deducted is:

$$\begin{aligned} & \sum_{c_j \in \mathcal{S}} \left(\eta + \sum_{k=2}^{\tau+1} 2^{k-2} \eta \right) \\ &= \sum_{c_j \in \mathcal{S}} 2^\tau \eta = |S| 2^\tau \frac{\sigma_*^2 t}{2^\tau |S| (|S| - t)} = \sigma_*^2 \frac{t}{|S| - t}. \end{aligned}$$

Thus, after the noise deduction, the remaining noise level at the aggregated update is exactly:

$$\sigma_*^2 \frac{|S|}{|S| - t} - \sigma_*^2 \frac{t}{|S| - t} = \sigma_*^2.$$

Case 2: Next, we consider the case where $|D| > 0$ clients drop. In this case, the total noise level that can be deducted is:

$$\sum_{c_j \in \mathcal{S} \setminus D} \sum_{k=2}^{\tau+1} 2^{k-2} \eta \mathbb{1}(b_{k-1} = 1) = \sum_{c_j \in \mathcal{S} \setminus D} \left[\frac{\lambda}{\eta} \right].$$

Denoting this quantity by m . On the one hand, we have:

$$\begin{aligned} m &= \sum_{c_j \in \mathcal{S} \setminus D} \left[\frac{\lambda}{\eta} \right] \eta \leq \sum_{c_j \in \mathcal{S} \setminus D} [\lambda] \leq \sum_{c_j \in \mathcal{S} \setminus D} \lambda \\ &= (|S| - |D|) \frac{(t - |D|) \sigma_*^2}{(|S| - t)(|S| - |D|)} = \sigma_*^2 \frac{t - |D|}{|S| - t}. \end{aligned}$$

Thus, the remaining noise level has a lower bound:

$$\sigma_*^2 \frac{|S| - |D|}{|S| - t} - m \geq \sigma_*^2 \frac{|S| - |D|}{|S| - t} - \sigma_*^2 \frac{t - |D|}{|S| - t} = \sigma_*^2.$$

On the other hand, we also have:

$$\begin{aligned} m &= \sum_{c_j \in \mathcal{S} \setminus D} \left[\frac{\lambda}{\eta} \right] \eta > \sum_{c_j \in \mathcal{S} \setminus D} \left(\frac{\lambda}{\eta} - 1 \right) \eta = \sum_{c_j \in \mathcal{S} \setminus D} (\lambda - \eta) \\ &= (|S| - |D|) \left(\frac{(t - |D|) \sigma_*^2}{(|S| - t)(|S| - |D|)} - \frac{\sigma_*^2 t}{2^\tau |S| (|S| - t)} \right) \\ &= (|S| - |D|) \frac{\sigma_*^2}{|S| - t} \left(\frac{t - |D|}{|S| - |D|} - \frac{t}{2^\tau |S|} \right) \\ &\geq (|S| - |D|) \frac{\sigma_*^2}{|S| - t} \left(\frac{t - |D|}{|S| - |D|} - \frac{1}{|S|} \right) \\ &= \frac{\sigma_*^2}{|S| - t} \left(t - |D| - \frac{|S| - |D|}{|S|} \right) \geq \frac{\sigma_*^2}{|S| - t} (t - |D| - 1). \end{aligned}$$

Thus, after noise deduction, the remaining noise level also has an upper bound:

$$\begin{aligned} & \sigma_*^2 \frac{|S| - |D|}{|S| - t} - m \\ &< \sigma_*^2 \frac{|S| - |D|}{|S| - t} - \frac{\sigma_*^2}{|S| - t} (t - |D| - 1) \\ &= \sigma_*^2 \frac{|S| - |D|}{|S| - t} - \sigma_*^2 \frac{t - |D|}{|S| - t} + \frac{\sigma_*^2}{|S| - t} = \sigma_*^2 + \frac{\sigma_*^2}{|S| - t}. \end{aligned}$$

\square

F Optimizing Data Chunking for Pipelining

Recall from §6.2 that m is the number of chunks specified by the pipeline execution plan, l_s is the predicted latency of executing a stage s for any data chunk (note that each chunk has an equal size). Moreover, denote by a the total number of stages in the distributed DP workflow, $b_{s,c}$, $f_{s,c}$ the beginning and finishing time of stage $s \in [a]$ for chunk $c \in [m]$, respectively. To find the optimal number of chunks, m^* , Hyades solves the following optimization problem which minimizes the end-to-end latency l , which equates to the finishing time of the last stage for the last chunk, i.e., $f_{a,m}$:

$$m^* = \arg \min_{m \in \mathbb{N}_+} f_{a,m},$$

$$\text{s.t. } f_{s,c} = b_{s,c} + l_s$$

$$b_{s,c} = \max\{o_{s,c}, r_{s,c}\},$$

$$o_{s,c} = \begin{cases} 0, & \text{if } s = 0, \\ f_{s-1,c}, & \text{otherwise,} \end{cases} \quad (18)$$

$$r_{s,c} = \begin{cases} 0, & \text{if } s = 0 \text{ and } c = 0, \\ f_{q,m} \text{ or } \perp, & \text{if } s \neq 0 \text{ and } c = 0, \\ f_{s,c-1}, & \text{otherwise,} \end{cases} \quad (19)$$

Table 4: The programming interface provided for developers to customize their own distributed DP algorithms and applications.

Category	Base Class	Customization Instruction
Distributed DP	ProtocolServer	Overwrite <code>set_graph_dict()</code> to specify the distributed DP workflow for pipeline plan generation. Create one method for coordinating each operation, e.g., <code>encode_data()</code> to instruct DP encoding.
	ProtocolClient	Overwrite <code>set_routine()</code> to specify the handler for each server’s request. Create one method for processing each server’s request, e.g., <code>encode_data()</code> to encode local input on request.
	DPHandler	Overwrite <code>init_params()</code> to specify how to initialize DP parameters, <code>encode_data()</code> and <code>decode_data()</code> to how to perform DP encoding and decoding given a chunk of input, respectively.
	AEHandler, KAHandler, PGHandler, SSHHandler	Overwrite the respective functionality for necessary security primitives: authenticated encryption, key agreement, pseudorandom generator, and secret sharing.
Application	AppServer	Overwrite <code>use_output()</code> to specify how the server uses the output of distributed DP.
	AppClient	Overwrite <code>prepare_data()</code> and <code>use_output()</code> to specify how a client prepares the input and consumes the output of distributed DP, respectively.

where $q = \max_{i < s} \{i \mid r_i = r_s\}$ where r_s is the dominant resource of stage s .⁴ Note that constraint 18 is enforced as each chunk needs to sequentially go through the execution of all stages. Constraint 19 is enforced for achieving another two principles in the meantime: 1) each resource can be allocated at most one chunk to execute a stage at any time, and 2) allocating resource r to execute stage s for a chunk c will be suspended, if there exists another chunk c' which has not finished its execution of some previous stage $q < s$ that also uses the resource r . This optimization problem can be solved by enumeration provided that all l_s ’s have been profiled.

G Generic Programming Interface

Support for Diverse Distributed DP Algorithms. As mentioned in Section 7, developers can implement customized distributed DP algorithms by leveraging the generic programming interface offered by Hyades. Specifically, Table 4 shows the base classes that are ready for customization.

The first base class, `ProtocolServer`, can be instantiated to implement different *server-end workflow* (like the one listed in Table 2). To help developers focus on developing the computation logic, Hyades provides them with established communication primitives (that are based on `Socket.IO` [5]) to which they can delegate the server-client interactions. For ease of specifying the execution order and resource dependencies of different operations, Hyades further provides the `set_graph_dict()` method where developers can annotate to help Hyades plan the optimal pipeline acceleration (§6.2). Similarly, for implementing *client-end workflow*, Hyades supplies developers with the base class `ProtocolClient` to customize. Also, Hyades provides the method `set_routine()` for developers to specify which part of the client workflow is triggered by a specific server request.

Apart from the high-level workflow construction, Hyades also provides developers with generic base classes to implement their own *privacy and security primitives*, including but not limited to differential privacy mechanisms (`DPHandler`), authenticated encryption schemes (`AEHandler`), key agree-

ment protocols (`KAHandler`), pseudorandom number generators (`PGHandler`), and secret sharing algorithms (`SSHHandler`). This enables developers to easily plug in and experiment with diverse privacy and security building blocks.

Support for Diverse Applications. As indicated in Table 4, Hyades also enables developers to readily port the aggregation framework to fuel other privacy-sensitive applications beyond FL. Specifically, developers can inherit the `AppServer` class with the `use_output()` method overwritten to specify how the aggregated result is consumed by the server. Similarly, they can also instantiate their own `AppClient` with 1) the method `prepare_data()` overwritten to define how a client’s data is produced, as well as 2) the method `use_output()` to configure how the aggregated result is consumed by the client. We will open-source Hyades and hereby invite the community to contribute more to privacy-preserving data analytics research.

⁴We abort the second case in Constraint 19 if such q does not exist.